

Heavy Flavor Hadrons in Statistical Hadronization of Strangeness-rich QGP

Inga Kuznetsova and Johann Rafelski

Department of Physics, University of Arizona, Tucson, Arizona, 85721, USA

(Dated: June 28, 2006)

We study b, c quark hadronization from QGP. We obtain the yields of charm and bottom flavored hadrons within the statistical hadronization model. The important novel feature of this study is that we take into account the high strangeness and entropy content of QGP, conserving strangeness and entropy yields at hadronization.

PACS numbers: 25.75.Nq, 12.38.Mh, 25.75.-q, 24.10.Pa

I. INTRODUCTION

A relatively large number of hadrons containing charmed and bottom quarks are expected to be produced in heavy ion (AA) collisions at the Large Hadrons Collider (LHC). Because of their large mass c, \bar{c}, b, \bar{b} quarks are produced predominantly in primary parton-parton collisions [1], at RHIC [2], and thus even more so at LHC. These heavy flavor quarks participate in the evolution of the dense QCD matter from the beginning. In view of the recent RHIC results it can be hoped that their momentum distribution could reach approximate thermalization within the dense QGP phase [3].

In our approach we will tacitly assume that the following evolution stages are present in heavy-ion collisions:

1. Primary partons collide producing c, b quarks;
2. A thermalized parton state within $\tau = \tau_{th} \simeq 0.25 - 1$ fm/c is formed. By the end of this stage nearly all entropy is produced.
3. The subsequent chemical equilibration: diverse thermal particle production reactions occur, allowing first the approach to chemical equilibrium by gluons g and light non strange quarks $q = u, d$.
4. The strangeness chemical equilibration within $\tau \sim 5$ fm/c).
5. The hadronization to final state near $\tau \sim 10$ fm/c).

It is important to observe that in the presence of de-confined QGP phase heavy hadrons containing more than one heavy quark are made from heavy quarks created in different initial NN collisions. Therefore yields of these hadrons are expected to be enhanced as compared to yields seen in single NN collisions [4, 5]. We note that the $Bc(b\bar{c}, \bar{b}c)$ and $J/\Psi(c\bar{c})$ and more generally all bound $c\bar{c}$ states yields were calculated before in the kinetic formation and dissociation models [4, 6]. Our present work suggests that it is important to account for the binding of heavy flavor with strangeness, an effect which depletes the eligible supply of heavy flavor quarks which could form $Bc(b\bar{c}, \bar{b}c)$ and $J/\Psi(c\bar{c})$ [7].

Enhanced production yield of multi-heavy hadrons can be considered to be an indicator of the presence of de-confined QGP phase for reasons which are analogue to

those of multi-strange (anti) baryons [8]. Considering that we have little doubt that QGP is the state of matter formed in the very high energy AA interactions, the study of yields of multi-heavy hadrons is primarily explored in this work in order to falsify, or justify, features of the statistical hadronization model (SHM) employed or the model itself in the context of formation of the heavy flavor hadrons.

For example, differing from other recent studies which assume that the hadron yields after hadronization are in chemical equilibrium [5, 9], we form the yields based on abundance of u, d, s quark pairs as these are available at the chemical freeze-out (particle formation) conditions in the quark-gluon phase. This approach is justified by the expectation that in a fast break-up of the QGP formed at RHIC and LHC the phase entropy and strangeness will be nearly conserved during the process of hadronization. We will investigate in quantitative terms how such chemical non-equilibrium yields, in the conditions we explore well above the chemical equilibrium abundance, influence the expected yields of single, and multi-heavy flavor hadrons.

In order to evaluate yields of final state hadrons we enforce conservation of entropy, and the flavor s, c, b quark pair number during phase transition or transformation. The faster the transition, the less likely it is that there is significant change in strange quark pair yield. Similarly, any entropy production is minimized when the entropy rich QGP breakup into the entropy poor HG occurs rapidly. The entropy conservation constraint fixes the final light quark yield. assume a fast transition between QGP and HG phases, such that all hadron yields are at the same physical conditions as in QGP breakup.

In the evaluation of heavy particle yields we form ratios involving e.g. as normalizer the total heavy flavor yield, such that the result we consider is little dependent on the unknown total yield of charm and bottom at RHIC and LHC. However, in some of the results we consider, in particular those related to the yields of multi-heavy hadrons, the total yields of charm and bottom we consider matter somewhat. The results we present are obtained for an assumed charm and bottom quark multiplicity:

$$\begin{aligned} \frac{dN_c}{dy} \equiv c &= 10, \\ \frac{dN_b}{dy} \equiv b &= 1. \end{aligned}$$

In certain situations we will explore how variation of this baseline yield impact the results. We note that the number of b quarks can not change during expansion, because of large mass $m_b \gg T$. It is nearly certain that all charm in QGP at RHIC is produced in the first parton collisions, for further discussion of LHC see Ref.[10] – it appears that for all practical purposes also in the more extreme thermal conditions at LHC charm is produced in the initial parton interactions.

In order to form physical intuition about the prevailing conditions in the QGP phase at time of hadronization, we also evaluate the heavy quark chemical reference density, that is the magnitude of the chemical occupancy factor in QGP, considering the pre-established initial yields of c and b from parton collision. For this purpose we use in the deconfined QGP phase:

$$\begin{aligned} m_c &= 1.2 \text{ GeV}, \\ m_b &= 4.2. \text{ GeV} \end{aligned}$$

We also take $\lambda_i = 1, i = u, d, s$ for all light flavors, since the deviation from particle-antiparticle yield symmetry is rather small and immaterial in the present discussion.

When computing the yields of charmed (and bottom) mesons we will distinguish only strange and non-strange abundances, but not charged with non charged (e.g. $D^-(\bar{c}d)$ with $\bar{D}^0(\bar{c}u)$). We assume that the experimental groups reporting results, depending on which type of D-meson were observed, can infer the total yield (charged+non-charged) which we present. We treat in similar way other heavy hadrons, always focusing on the heavy and the strange flavor content and not distinguishing the light flavor content.

Our paper is organized as follows: we first introduce the elements of the SHM model we use to evaluate heavy flavor hadron yields in section II. Turning to the results obtained in this paper, we first discuss the relative yields of strange and non-strange heavy mesons in section III, and show how this relates the value of the strangeness chemical (non)equilibrium parameters. In this context, we also propose a multi particle ratio as a measure of the hadronization temperature, and explore how a multi-temperature, staged, freeze-out would impact the relevant results.

The main body of our work is found in section IV, where we study the yields of heavy and multi-heavy hadrons, and compare when appropriate to the chemical equilibrium results. We begin with a study of the charm and bottom quark phase space occupancy parameters (subsection IV A) and turn in subsection IV B to discussion of the yields of single heavy mesons, which we follow with discussion of yields of single heavy baryons in subsection IV C. We then present the expected yields of the multi-heavy hadrons, in so far these can be considered in the grand canonical approach. We conclude our work with a brief summary in section V.

Throughout this paper we use explicitly and implicitly the properties of QGP fireball and of hadron phase space

regarding entropy content and strangeness. These are assembled in the appendices A for entropy and B for strangeness. We consider the entropy in a system with evolving strangeness in appendix A 2 and show that the number of active degrees of freedom in a QGP is nearly constant. Another highlight is the discussion of sudden hadronization of strangeness and the associated values of hadron phase space parameters in appendix B 3.

II. STATISTICAL HADRONIZATION MODEL (SHM)

SHM arises from the Fermi multi particle production model [11]. Fermi considered that all hadron production matrix elements are saturated to unity. This allows the use of the Fermi golden rule with the N-particle phase space to obtain the relative particle yields. In modern language this is SHM in micro-canonical ensemble, micro-canonical implies that discrete (flavor) quantum numbers and the energy are conserved exactly.

The transition from micro-canonical to canonical, and grand-canonical ensembles simplifies the computational effort considerably [12]. This important step does not in our context introduce the hadron phase, although before the understanding of QGP this of course was the reaction picture: a highly compressed hadron gas matter evaporates particles. Today, it is the highly compressed hot quark-gluon matter that evaporates particles. In principle, there is no necessity to introduce a hadron gas phase of matter in order to use SHM to describe particle production.

On the other hand, in order to understand the physical meaning of the parameters introduced to describe hadron phase space in grand-canonical ensemble, such as temperature T , it is quite convenient to *imagine* the existence of the hadron phase which follows the QGP phase. This can be taken to the extreme, and a long lasting, chemically equilibrating phase of hadrons can be assumed, that follows in time the formation of the QGP fireball. Such a reaction picture may not agree with the fast evolving circumstance of a heavy ion collision. One should note that the study of hot hadron matter on the lattice within the realm of L-QCD involves at all times a fully equilibrated system. This will in key features differ from the non-equilibrium QGP properties accompanying the hadronization process.

The important parameters of the SHM, which control the relative yields of particles, are the particle specific fugacity factor λ and space occupancy factor γ . The fugacity is related to chemical potential $\mu = T \ln \lambda$. The occupancy γ is, nearly, the ratio of produced particles to the number of particle expected in chemical equilibrium. The actual momentum distribution is:

$$\frac{d^6 N}{d^3 p d^3 x} \equiv f(p) = \frac{g}{(2\pi)^3} \frac{1}{\gamma^{-1} \lambda^{-1} e^{E/T} \pm 1} \rightarrow \gamma \lambda e^{-E/T}, \quad (1)$$

where the Boltzmann limit of the Fermi ‘(+)’ and Bose ‘(−)’ distributions is indicated, g is the degeneracy factor, T is the temperature and $E = E(p)$ is the energy.

The fugacity λ is associated with a conserved quantum number, such as net-baryon number, net-strangeness, heavy flavor. Thus antiparticles have inverse value of λ , and λ evolution during the reaction process is related to the changes in densities due to dynamics such as expansion. γ is the same for particles and antiparticles. Its value changes as a function of time even if the system does not expand, for it describes buildup of the particular particle species. For this reason γ is changes rapidly during the reaction, while λ is more constant. Thus it is γ which carries the information about the time history of the reaction and the precise condition of particle production referred to as chemical freeze-out.

The number of particles of type ‘ i ’ with mass m_i per unit of rapidity is in our approach given by:

$$\frac{dN_i}{dy} = \gamma_i n_i^{\text{eq}} \frac{dV}{dy}. \quad (2)$$

Here dV/dy is system volume associated with the unit of rapidity, and n_i^{eq} is a Boltzmann particle density in chemical equilibrium:

$$\begin{aligned} n_i^{\text{eq}} &= g_i \int \frac{d^3 p}{(2\pi)^3} \lambda_i \exp(-\sqrt{p^2 + m_i^2}/T) \\ &= \lambda_i \frac{T^3}{2\pi^2} g_i W(m_i/T), \end{aligned} \quad (3)$$

and

$$W(x) = x^2 K_2(x) \rightarrow 2 \text{ for } x \rightarrow 0. \quad (4)$$

Both, $m_i c^2 \rightarrow m_i$, and $kT \rightarrow T$, are measured in energy units when $\hbar, c, k \rightarrow 1$.

For the case of heavy flavors $m \gg T$, the dominant contribution to the Boltzmann integral Eq. (3) arises from $p \simeq \sqrt{2mT}$, we do not probe the tails of the momentum distribution. Thus even when the momentum distribution is not well thermalized, the yield of heavy flavor hadrons can be described in term of the thermal yields, Eq.(2), where:

$$\begin{aligned} n_i^{\text{eq}} &= \frac{g_i T^3}{2\pi^2} \lambda_i \sqrt{\frac{\pi m_i^3}{2T^3}} \exp(-m_i/T) \times \\ &\quad \times \left(1 + \frac{15T}{8m_i} + \frac{105}{128} \left(\frac{T}{m_i} \right)^2 \dots \right). \end{aligned} \quad (5)$$

Often we can use the first term alone for heavy flavor hadrons, since $T/m \ll 1$, however the series in Eq. (5) converges slowly and one should proceed with caution.

We use occupancy factors γ_i^Q and γ_i^H for QGP and hadronic gas phase respectively, tracking every quark flavor ($i = q, s, b, c$) . We assume that in the QGP phase the light quarks and gluons are adjusting fast to the ambient conditions, and thus are in chemical equilibrium

with $\gamma_{q,G}^Q \rightarrow 1$. For heavy, and strange flavor, the value of γ_i^Q at hadronization condition is given by the number of particles present, generated by prior kinetic processes, see Eq. (2).

The yields of different quark flavors originate in different physical processes, such as production in initial collisions for c, b, s , and for s also production in thermal plasma processes. In general we thus cannot expect that $\gamma_{c,b}^Q$ will be near unity at hadronization. However, the thermal strangeness production process $GG \rightarrow s\bar{s}$ can nearly chemically equilibrate strangeness flavor in plasma formed at RHIC and/or LHC [10], and we will always consider, among other cases the limit $\gamma_s^Q \rightarrow 1$ prior to hadronization.

The yields of all hadrons after hadronization are also given by Eq. (2), which helps us to obtain γ_i^H for hadrons. In general, evaluation of hadron chemical parameters presents a more complicated case since they are composed from those of valance quarks in the hadron (three quarks, or a quark and anti quark). Therefore, in the coalescence picture, the phase space occupancy γ^H of hadrons will be the product of γ^H ’s for each constituent quark. For example for the charmed meson D ($c\bar{q}$)

$$\gamma_D^H = \gamma_c^H \gamma_q^H. \quad (6)$$

To evaluate yields of final state hadrons we enforce conservation of entropy, and the flavor s, c, b quark pair number during phase transition or transformation. The faster the transition, the less likely is that there is significant change in strange quark pair yield. Similarly, any entropy production is minimized when the entropy rich QGP breakup into the entropy poor HG occurs rapidly. The entropy conservation constraint fixes the final light quark yield. We assume a fast transition between QGP and HG phases, such that all hadron yields are at the same physical conditions as in QGP breakup.

Assuming that in the hadronization process the number of b, c, s quark pairs doesn’t change, the three unknown $\gamma_s^H, \gamma_c^H, \gamma_b^H$ can be determine from their values in the QGP phase, $\gamma_s^Q, \gamma_c^Q, \gamma_b^Q$ and the three flavor conservation equations,

$$\frac{dN_i^H}{dy} = \frac{dN_i^Q}{dy} = \frac{dN_i}{dy}, \quad i = s, c, b. \quad (7)$$

In order to conserve entropy:

$$\frac{dS^H}{dy} = \frac{dS^Q}{dy} = \frac{dS}{dy}, \quad (8)$$

a value $\gamma_q^H \neq 1$ is allowed for, while the value in the QGP phase $\gamma_{q,G}^Q = 1$. This implies that yields of hadrons with light quark content are in general not in chemical equilibrium. This influences the yields of heavy flavored particles in final state as we shall discuss below.

As noted at the beginning of this section, the use of the hadron phase space (denoted by H above) does not imply

the presence of a real physical ‘hadron matter’ phase: the SHM particle yields will be attained solely on the basis of availability of this phase space as noted at the beginning of this section. Another way to argue this is to imagine a pot of quark matter with hadrons evaporating. Which kind of hadron emerges and at which momentum is entirely determined by the access to the phase space, and there are only free-streaming particles in the final state.

Thinking in these terms, one can imagine that especially for heavy quark hadrons some particles are pre-formed in the deconfined plasma, and thus the heavy hadron yields may be based on a value of temperature which is higher than the global value expected for other hadrons. For this reason we will study in this work a range $140 < T < 260$ MeV and also consider sensitivity to this type of two-temperature chemical freeze-out of certain heavy hadron yield ratios.

III. RELATIVE CHARMED HADRON YIELDS

A. Determination of γ_s^H/γ_q^H

We have seen considering s/S and also s and S individually across the phase limit (App. A, B) that in general one would expect chemical non-equilibrium in hadronization of chemically equilibrated QGP. We first show that this result matters for the relative charm meson yield ratio D_s/D , where $D_s(c\bar{s})$ comprises all mesons of type $(c\bar{s})$ which are listed in the bottom section of table I, and $D(c\bar{q})$ comprise yields of all $(c\bar{q})$ states listed in the top section of table I. This ratio is formed based on the assumption that on the time scale of strong interactions the family of strange-charmed mesons can be distinguished from the family non-strange charmed mesons.

The yield ratio D_s/D is shown in figure 1. It is proportional to γ_s^H/γ_q^H and weakly dependent on T :

$$\frac{D_s}{D} \approx \frac{\gamma_s^H \sum_i g_{Dsi} m_{Dsi}^{3/2} \exp(-m_{Dsi}/T)}{\gamma_q^H \sum_i g_{Di} m_{Di}^{3/2} \exp(-m_{Di}/T)} = f(T) \frac{\gamma_s^H}{\gamma_q^H}. \quad (9)$$

A deviation of γ_s^H/γ_q^H from unity in the range we found in previous section B 3 leads to a noticeable difference in the ratio D_s/D . We show in figure 1 results for $T = 140, 160, 180$ MeV. In this temperature range the effect due to $\gamma_s^H/\gamma_q^H \neq 1$ is the dominant contribution to the variation of this relative yield.

B. Check of statistical hadronization model

We next construct a heavy flavor particle ratio that depends on hadronization temperature only. To cancel the fugacities and the volume we consider the ratio $J/\Psi\phi/D_s\bar{D}_s$ in figure 2. Here J/Ψ yield includes the yield of $(c\bar{c})$ mesons decaying into the J/Ψ . All phase space occupancies cancel since $J/\Psi \propto \gamma_c^H \gamma_s^H$, $\phi \propto \gamma_s^H \gamma_q^H$, $D_s \propto \gamma_c^H \gamma_s^H$

TABLE I: Open charm, and bottom, hadron states we considered. States in parenthesis either need confirmation or have not been observed experimentally, in which case we follow the values of Refs. [13, 14]. We have charm-bottom symmetry required for certain observables.

	hadron	M[GeV]	hadron	M[GeV]	g
D	$D^0(0^-)$	$c\bar{u}$	$B^0(0^-)$	$b\bar{u}$	5.279
	$D^+(0^-)$	$c\bar{d}$	$B^+(0^-)$	$b\bar{d}$	5.279
	$D^{*0}(1^-)$	$c\bar{u}$	$B^{*0}(1^-)$	$b\bar{u}$	5.325
	$D^{*+}(1^-)$	$c\bar{d}$	$B^{*+}(1^-)$	$b\bar{d}$	5.325
	$D^0(0^+)$	$c\bar{u}$	$B^0(0^+)$	$b\bar{u}$	5.697
	$D^+(0^+)$	$c\bar{d}$	$B^+(0^+)$	$b\bar{d}$	5.697
	$D_1^{*0}(1^+)$	$c\bar{u}$	$B_1^{*0}(1^+)$	$b\bar{u}$	5.720
	$D_1^{*+}(1^+)$	$c\bar{d}$	$B_1^{*+}(1^+)$	$b\bar{d}$	5.720
	$D_2^{*0}(2^+)$	$c\bar{u}$	$B_2^{*0}(2^-)$	$b\bar{u}$	(5.730)
	$D_2^{*+}(2^+)$	$c\bar{d}$	$B_2^{*+}(2^+)$	$b\bar{d}$	(5.730)
D_s	$D_s^+(0^-)$	$c\bar{s}$	$B_s^0(0^-)$	$s\bar{b}$	5.3696
	$D_s^{*+}(1^-)$	$c\bar{s}$	$B_s^{*0}(1^-)$	$s\bar{b}$	5.416
	$D_{sJ}^{*+}(0^+)$	$c\bar{s}$	$B_{sJ}^{*0}(0^+)$	$s\bar{b}$	(5.716)
	$D_{sJ}^{*+}(1^+)$	$c\bar{s}$	$B_{sJ}^{*0}(1^+)$	$s\bar{b}$	(5.760)
	$D_{sJ}^{*+}(2^+)$	$c\bar{s}$	$B_{sJ}^{*0}(2^+)$	$s\bar{b}$	(5.850)

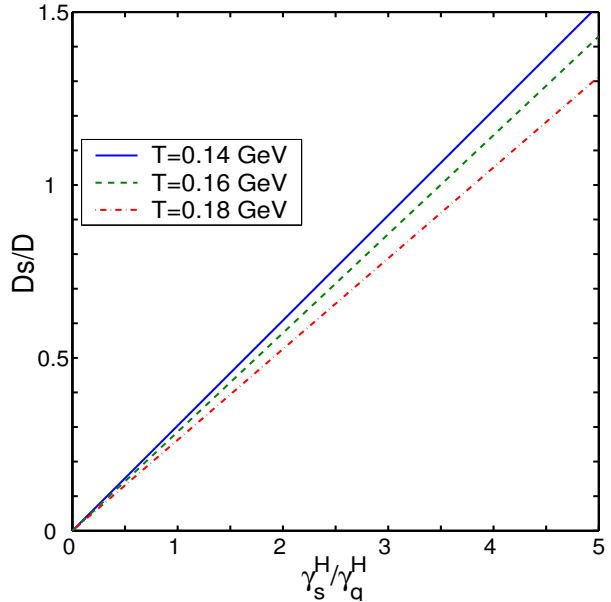


FIG. 1: (Color on line) D_s/D ratio as a function of γ_s^H/γ_q^H for $T=140$ MeV (blue, solid line), $T=160$ MeV (green, dashed line) and $T=180$ MeV (red, dash-dot line).

and similarly $\bar{D}_s \propto \gamma_c^H \gamma_s^H$. When using here the particle $D_s(c\bar{s})$ and antiparticle $\bar{D}_s(c\bar{s})$ any chemical potentials present are canceled as well. However, for the LHC and even RHIC environments this refinement is immaterial.

This ratio $J/\Psi\phi/D_s\bar{D}_s$, turns out to be practically constant, within a rather wide range of hadronization temperature T , see figure 2. The temperature range we study $140 < T < 280$ MeV allows us to consider an early freeze-out of different hadrons. To be sure of the temperature independence of $J/\Psi\phi/D_s\bar{D}_s$ we next consider the possibility that hadronization temperature T of

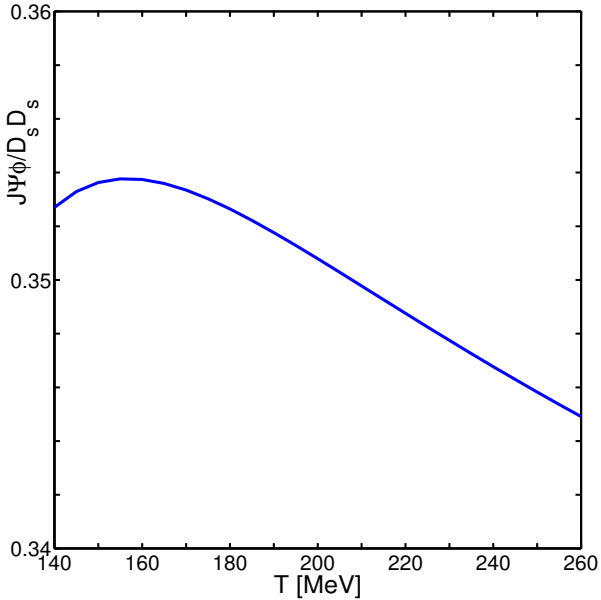


FIG. 2: (Color on line) $J/\Psi \phi / D_s \bar{D}_s$ ratio as a function of hadronization temperature T .

charmed hadrons is higher than hadronization temperature T_0 of ϕ . We study this question by exploring the sensitivity of the ratio $J/\Psi \phi / D_s \bar{D}_s$ to the two temperature freeze-out in figure 3, see bottom three lines for $T_0 = 180, 160, 140$ MeV. There is even less variation with temperature now, with the result considered as function of $-40 < T - T_0 < 100$ MeV. If this were to be measured as experimental result,

$$\frac{J/\Psi \phi}{D_s \bar{D}_s} \simeq 0.35, \quad (10)$$

one could not but conclude that all particles involved are formed by mechanism of statistical hadronization.

This interesting result can be understood, considering the behavior of the $\gamma_s(T_0)/\gamma_s(T)$ ratio, which increases rapidly with increasing $T - T_0$ (see the top three lines in figure 3) which compensates the change in ϕ -yield, an effect we already encountered in the context of the results seen in figure 16.

IV. YIELDS OF HEAVY FLAVORED HADRONS

A. Phase space occupancy γ_c^H and γ_b^H

The first step in order to determine the yields of heavy flavor hadronic particles is the determination of the phase space occupancy γ_c^H and γ_b^H . γ_c^H is obtained from equality of number of these quarks (i.e. of quark and anti quark pairs) in QGP and HG. The yield constraint is:

$$\frac{dN_c}{dy} = \frac{dV}{dy} [\gamma_c^H n_{op}^c + \gamma_c^H (n_{hid}^{eq} + 2\gamma_q^H n_{ccq}^{eq} + 2\gamma_s^H n_{ccs}^{eq})]; \quad (11)$$

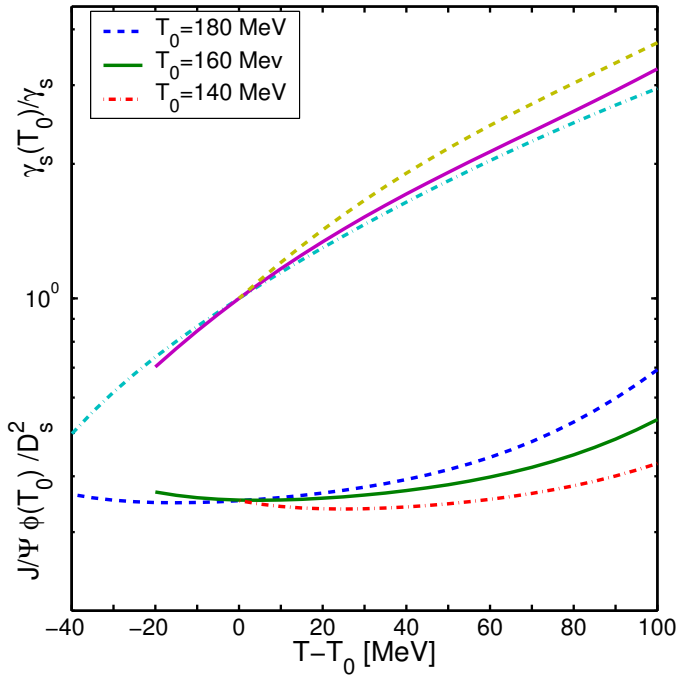


FIG. 3: (Color on line) $J/\Psi \phi(T_0)/D_s D_s$ ratio evaluated at two temperatures, T for heavy flavor hadrons, and T_0 for ϕ as function of $T - T_0$, with three values of $T_0 = 140, 160, 180$ MeV considered.

where open ‘op’ charm yield is:

$$n_{op}^c = \gamma_q^H n_D^{eq} + \gamma_s^H n_{D_s}^{eq} + \gamma_q^H n_{qqc}^{eq} + \gamma_s^H \gamma_q^H n_{sqc}^{eq} + \gamma_s^H n_{ssc}^{eq}. \quad (12)$$

Here n_D^{eq} and $n_{D_s}^{eq}$ are densities of D and D_s mesons, respectively, in chemical equilibrium, n_{qqc}^{eq} is equilibrium density of baryons with one charm and two light quarks, n_{ssc}^{eq} is density of baryons with one charm (or later on one bottom quark) and two strange quarks (Ω_c^0, Ω_b^0) and n_{hid}^{eq} is equilibrium particle density with both, a charm (or bottom) and an anticharm (or antibottom) quark ($C=0, B=0, S=0$). γ_c^H can be obtained from this equation.

Similar calculations can be done for γ_b^H . The only difference is that we need to add number of B_c mesons to the right hand side of (11),

$$\frac{dN_{B_c}}{dy} = \gamma_b^H \gamma_c^H n_{B_c}^{eq} \frac{dV}{dy}. \quad (13)$$

$n_{B_c}^{eq}$ is density in chemical equilibrium of B_c . In the calculation of γ_c^H the contribution of term with n_{B_c} is very small and we did not consider it above.

The value of γ_c is in essence controlled by the open single charm mesons and baryons. For this reason we do not consider the effect of exact charm conservation. The relatively small effects due to micro canonical phase space of charm are leading to a slight up-renormalization of the value of γ_c so that the primary dN_c/dy yield is preserved. This effect enters into the yields of multi-charmed and hidden charm hadrons, where the compensation is not

exact and there remains slight change in these yields. However, the error made considering the high yield of charm is not important. On the other hand for multi-bottom and hidden bottom hadrons micro-canonic effect can be large, depending on actual bottom yield, and thus we will not discuss in this paper yields of these hadrons, pending extension of the methods here developed to include canonical phase space effect.

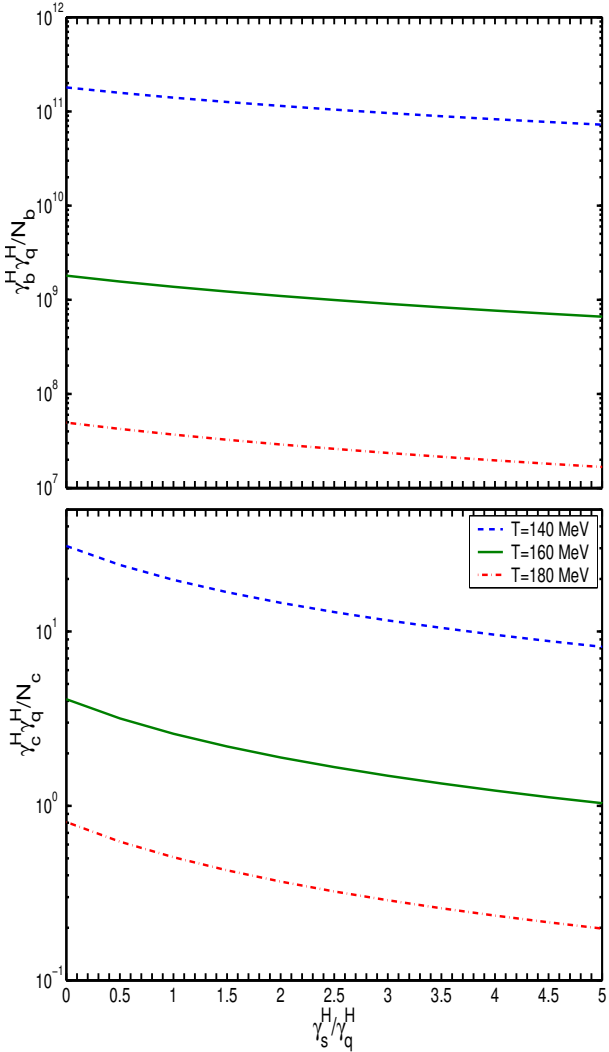


FIG. 4: (Color on line) $\gamma_c^H \gamma_q^H / N_c$ ratio as a function of γ_s^H / γ_q^H for $T=0.14$ GeV (blue, solid line), $T=0.16$ GeV (green, dashed line) and $T=0.18$ GeV (red, dash-dot line). Results for γ_q^H are from Fig.18.

In a good approximation, see Eq. (11), the value of $\gamma_{c,b}^H$ scales with the total yields $dN_{c,b}/dy$, except for immaterial corrections from the multi-heavy hadrons. Therefore, we show in figure 4 the relative dependence $\gamma_b^H \gamma_q^H / N_b$ (top) and $\gamma_c^H \gamma_q^H / N_c$ (bottom) on the chemical non equilibrium ratio γ_s^H / γ_q^H for several temperatures (from top to bottom) $T = 140, 160, 180$ MeV. We note the monotonic decrease with γ_s^H / γ_q^H . This is due to the fact that

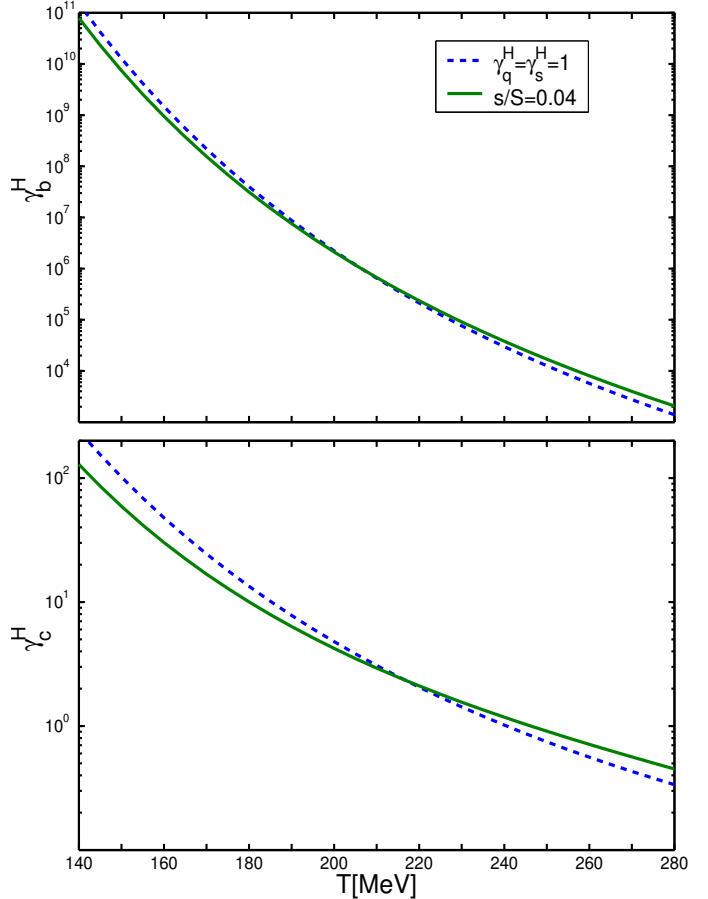


FIG. 5: (Color on line) $\gamma_b^H (b = 1)$ (upper panel), and γ_c^H (lower panel), as functions of temperature of hadronization T . The solid line is γ_c^H and γ_b^H non equilibrium for $s/S = 0.04$ and dashed line is equilibrium case $\gamma_s = \gamma_q = 1$.

with an increase of γ_s^H / γ_q^H there is more phase space for the available c quarks to bind to. This decrease of the value of the heavy flavor fugacity with γ_s^H / γ_q^H influences significantly the heavy flavor hadron yields of interest to us.

We can compare with the chemical equilibrium (dashed lines) setting $\gamma_s^H = \gamma_q^H = 1$ in Eq. (11). We consider the temperature dependence of both γ_b^H (top) and γ_c^H (bottom) in figure 5. In non-equilibrium case (solid lines) the space occupancy γ_s is obtained from Eq. (B4) and γ_q^H is chosen to keep $s/S = 0.04$. At hadronization condition $T = 160 \pm 20$ MeV temperatures we see in figure 5 a significant (considering the fast changing logarithmic scale) difference between the chemical equilibrium, and non-equilibrium results.

γ_b^H and γ_c^H are nearly proportional to the yields $dN_{b,c}/dy$. The deviation from the proportionality is due to the abundance of multi-heavy hadrons and is small. To estimate this effect more quantitatively we first eval-

uate:

$$\gamma_{c0}^H = \frac{dN_c}{dy} / \left(\frac{dV}{dy} n_{\text{open}}^c \right). \quad (14)$$

Next we compare with the result when we take into account the last three terms in Eq.(11). In the range of $dN_c/dy = (5, 30)$, γ_c^H/N_c changes at temperature $T = 140$ MeV by $\sim 6\%$ for the $s/S = 0.04$. For the chemical equilibrium case $\gamma_s = \gamma_q = 1$ γ_c^H/N_c changes up to 15% at the same conditions. The multiplicity dN_c/dy can also influence γ_b^H , since as we noted it also includes a term proportional $\gamma_c^H n_{Bc}^{\text{eq}}$. In the range of $N_c = (5, 30)$, γ_b/N_b changes at temperature $T = 0.14$ MeV by $\sim 0.5\%$ for $s/S = 0.04$. Since the mass of b -quark is much larger than that of c -quark, the effect due to multi-bottom states is negligible.

B. D, Ds, B, Bs meson yields

Considering Eq.(2), and using γ_c^H , γ_s^H , γ_q^H at a given T we have now all the inputs required to compute absolute and relative particle yields of all heavy hadrons which we can consider within the grand canonical phase space. When we consider chemical equilibrium case, we use naturally $\gamma_s^H = \gamma_q^H = 1$. In figure 6 as functions of hadronization temperature we show in the upper panel the fractional yields of charmed D/N_c and D_s/N_c mesons, and in the lower panel B/N_b and B_s/N_b . Fractional means that these yields are normalized by the total number of charm quarks N_c and, respectively bottom quarks N_b , and thus tell us how big a fraction of available heavy flavor quarks binds to non-strange and strange heavy mesons, respectively. The dashed and dash-dot lines were obtained for chemical equilibrium. The extreme upper and lower lines are for $s/S = 0.03$ (purple, solid and dot marked solid lines), while the central lines are for $s/S = 0.04$ (green, solid and dot marked lines). The yields D , B and D_s , B_s are sum over excited states of D , B and D_s , B_s respectively, see table I for the ‘vertical tower’ of resonances we have included.

We note that there is considerable symmetry at fixed T between the fractional yields of charmed, and bottom mesons, for the same condition of s/S . The chemical equilibrium results show significant difference between strange and non-strange heavy mesons. For non-equilibrium with increasing s/S and towards low T these yields become more symmetric. In the case of chemical equilibrium, for the considered very wide range of hadronization temperatures $D_s/N_c \simeq B_s/N_b \simeq 0.2$ are nearly constant. Any increase from this result would suggest presence of chemical non-equilibrium yield of strangeness.

The yields of D_s/N_c and B_s/N_b are very similar, and similarly so for D/N_c and B/N_b . Thus the relative yield of either of these mesons measures the relative yield of charm to bottom participating in the statistical

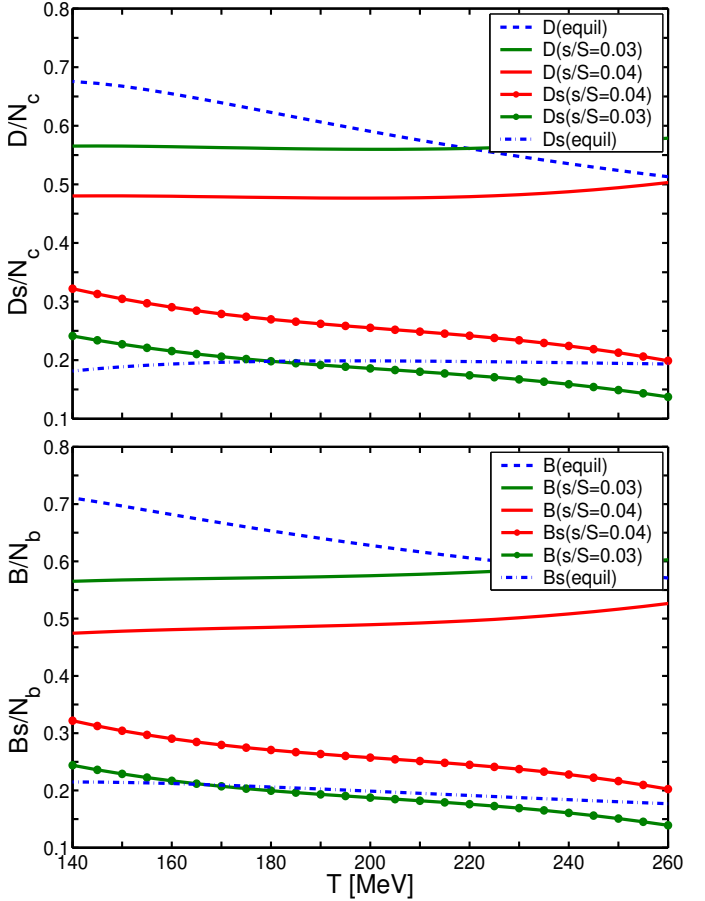


FIG. 6: (Color on line) Upper panel, fractional charm meson yield, and lower panel, fractional bottom meson yields. Equilibrium (dashed lines) and non equilibrium for $s/S = 0.03$ (purple) and $s/S = 0.04$ (green,) for D/N_c (solid line, upper panel); D_s/N_c (point marked solid line, upper panel); B/N_b (solid line, lower panel); and B_s/N_b (point marked solid line, lower panel), as function of T .

hadronization process:

$$\frac{D_s}{B_s} \simeq \frac{D}{B} = \frac{N_c}{N_b} \quad (15)$$

This is a very precise result, which somewhat depends on the tower of resonances included, and thus in particular on the symmetry in the heavy quark spectra between charmed and bottom states which we imposed.

We now turn to discuss ratios of non-strange to strange heavy mesons of the same (heavy) flavor, see figure 7. Charm is shown in upper panel and bottom flavor in lower panel as a function of T . We see that there is considerable symmetry in the relative yields between charmed and bottom mesons with upper and lower panels looking quasi-identical. Except for accidental values of T where the equilibrium results (blue, dashed lines) cross the fixed s/S results, there is considerable deviation in these ratios expected for strangeness chemical non equilibrium. If the heavy meson yields are estab-

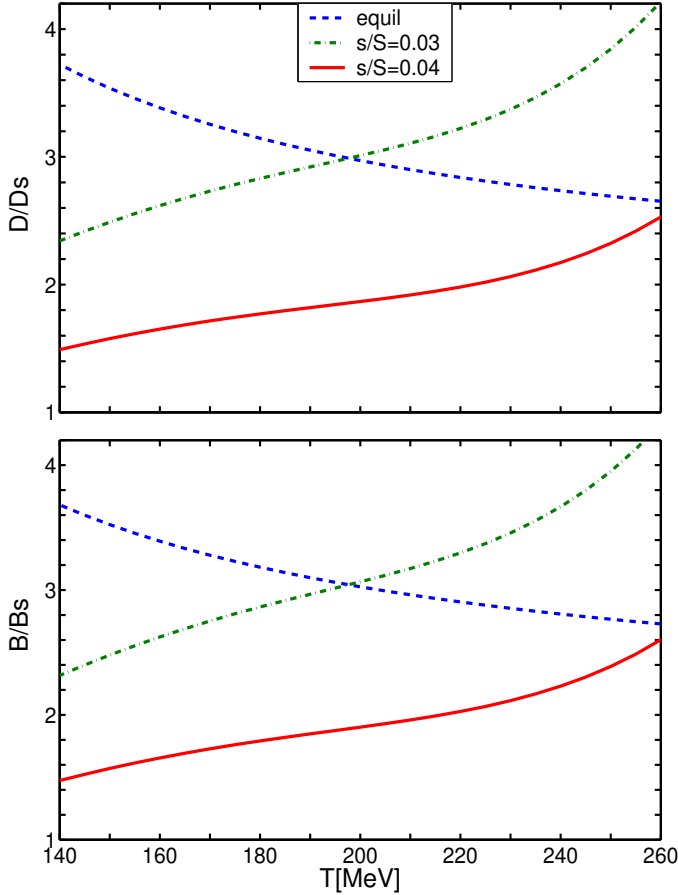


FIG. 7: (Color on line) Ratios D/D_s (upper panel) and B/B_s (lower panel) are shown as function of T for different s/S ratios and in chemical equilibrium. Solid line is for $s/S = 0.04$, dash-dot line is for $s/S = 0.03$, dashed line is for $\gamma_s^H = \gamma_s^H = 1$.

lished at temperatures similar to regular hadrons, relative enhancement by factor 2.5 in strange-heavy mesons is to be expected. For RHIC conditions $s/S = 0.03$ with $c = \bar{c} = 2$) D/D_s ratio become lower than chemical equilibrium value for $T < 0.2$ and this ratio decreases by factor of 1.5 for $T \rightarrow 140$ MeV.

C. Heavy baryon yields

As was the case comparing charm to bottom mesons we also establish a symmetric set of charmed and bottom baryons, shown in the table II. Many of the bottom baryons are result of theoretical studies and we include that many states to be sure that both charm and bottom are consider in perfect symmetry to each other. In figure 8 (upper panel) we show hadronization temperature dependencies of yields of baryons with one charm quark normalized to charm multiplicity N_c . We show separately yields of baryons without strange quark $(\Lambda_c + \Sigma_c)/N_c$, and with one strange quark $S=1$ (Ξ_c/N_c) for $s/S = 0.04$,

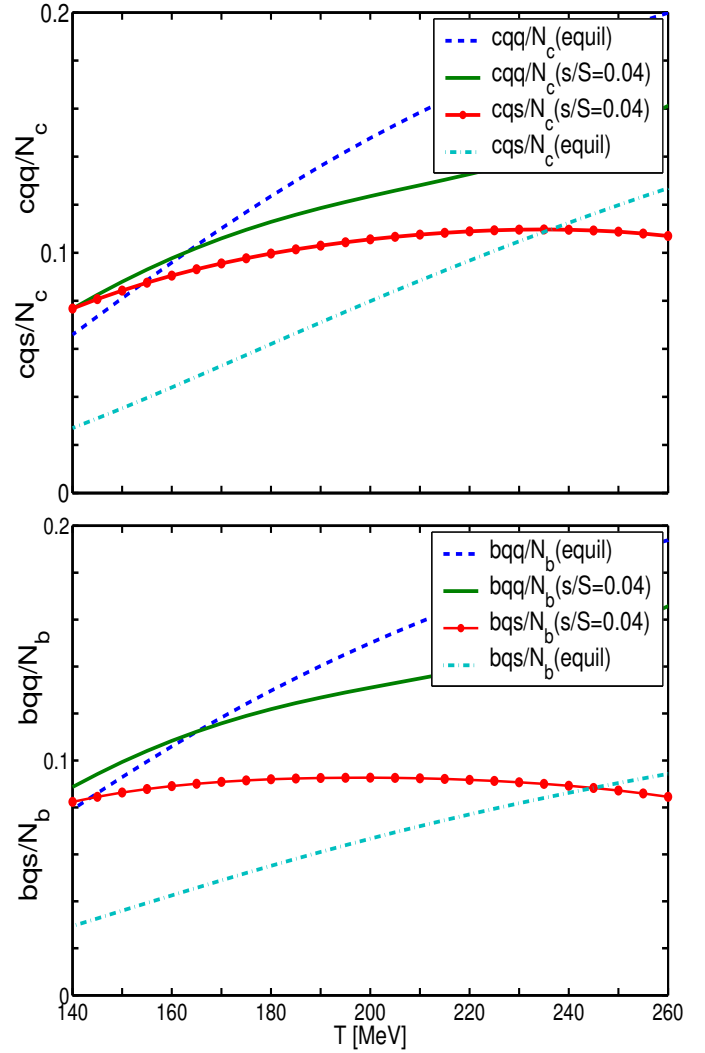


FIG. 8: (Color on line) Equilibrium (dashed and dash-dot) and non equilibrium (solid and dot marked lines) ratios (the upper panel) $(\Lambda_c + \Sigma_c)/N_c$ and Ξ_c/N_c (upper panel) and $(\Lambda_b + \Sigma_b)/N_b$ and Ξ_b/N_b (lower panel) as a function of T .

i.e. chemical strangeness non-equilibrium and for equilibrium case (solid and point marked lines). A similar result is presented for bottom baryons in the lower panel of figure 8. We note that the result for bottom baryons is more uncertain since most baryon masses entering are not experimentally verified.

In figure 9 we show ratios $cqq/cqs = (\Lambda_c + \Sigma_c)/\Xi_c$ (upper panel) and $bqq/bqs = (\Lambda_b + \Sigma_b)/\Xi_b$ (lower panel) for $s/S = 0.04$ (solid line) and chemical equilibrium (dashed line) case. In the case $s/S = 0.04$ the yield of strange charmed baryons is for a wide range of T similar to that of non-strange charmed baryons. At low hadronization temperature both yields (strange and non-strange charmed baryons) are practically equal. Lower panel shows the result for bottom baryons, where the behavior we see is almost the same as for charmed baryons.

The yield of multi-strange charmed baryon, $\Omega_c(css)$ is

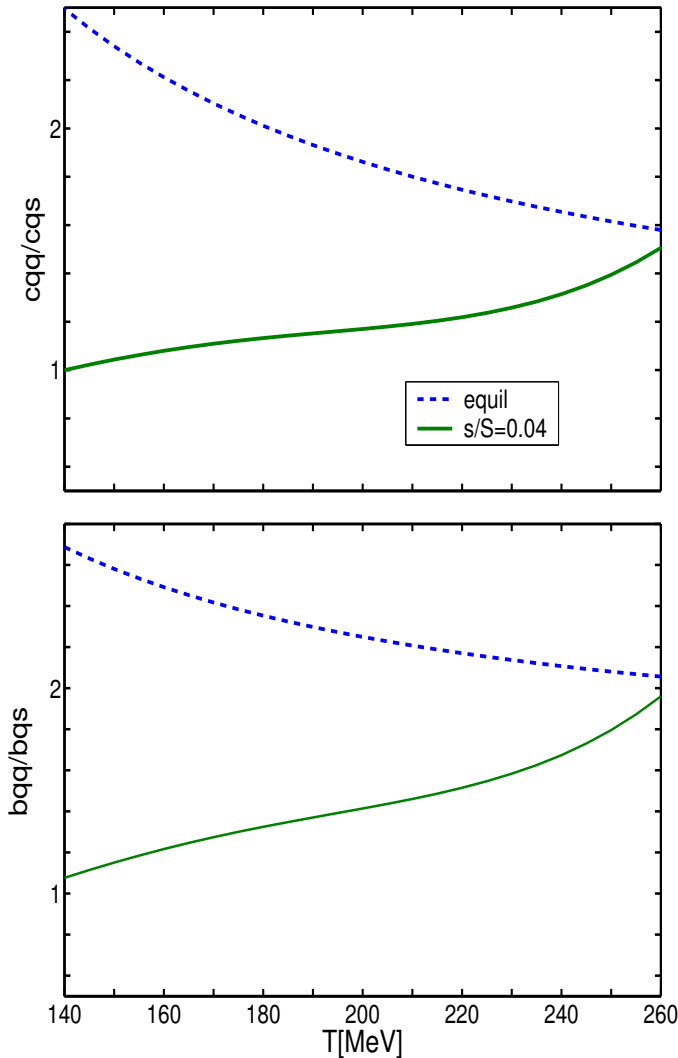


FIG. 9: (Color on line) Equilibrium (dashed (blue) line) and non equilibrium (solid (green) line) ratios $cqq/cqs = (\Lambda_c + \Sigma_c)/\Xi_c$ (upper panel) and $bqq/bqs = (\Lambda_b + \Sigma_b)/\Xi_b$ (lower panel) as a function of T .

TABLE II: Charm and bottom baryon states considered. States in parenthesis are not known experimentally and have been adopted from theoretical source [15].

hadron	M[GeV]	hadron	M[GeV]	g		
$\Lambda_c^+(1/2^+)$	udc	2.285	$\Lambda_b(1/2^+)$	udb	5.624	2
$\Lambda_c^+(1/2^-)$	udc	2.593	$\Lambda_b(1/2^-)$	udb	(6.000)	2
$\Lambda_c^+(3/2^-)$	udc	2.6266	$\Lambda_b(1/2^-)$	udb	(6.000)	2
$\Sigma_c^+(1/2^+)$	qqc	2.452	$\Sigma_b^0(1/2^+)$	qqb	(5.770)	6
$\Sigma_c^*(3/2^+)$	qqc	2.519	$\Sigma_b^{0*}(3/2^+)$	qqb	(5.780)	12
$\Xi_c(1/2^+)$	qsc	2.470	$\Xi_b(1/2^+)$	qsb	(5.760)	4
$\Xi_c'(1/2^+)$	qsc	2.5741	$\Xi_b'(1/2^+)$	qsb	(5.900)	4
$\Xi_c(3/2^+)$	qsc	2.645	$\Xi_b'(3/2^+)$	qsb	(5.900)	8
$\Omega_c(1/2^+)$	ssc	2.700	$\Omega_b(1/2^+)$	ssb	(6.000)	2
$\Omega_c(3/2^+)$	ssc	(2.700)	$\Omega_b(3/2^+)$	ssb	(6.000)	4

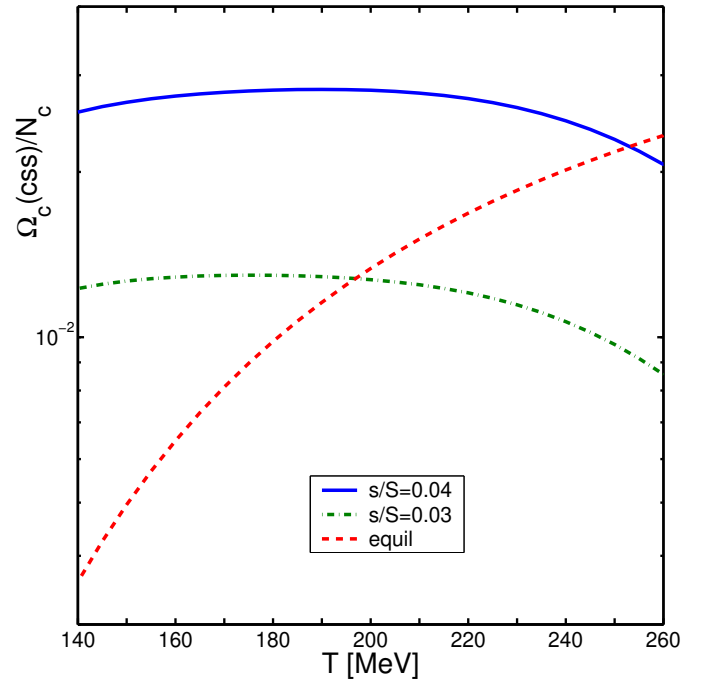


FIG. 10: (Color on line) Equilibrium (red, dashed line) and non equilibrium $s/S = 0.03$ (green, dot-dashed line), $s/S = 0.04$ (blue, solid line) fractional yield $\Omega_c(css)/N_c$ as function of T .

similar to the light multi-strange hadrons much more sensitive to strangeness non-equilibrium. In figure 10 we see a large increase in fractional yield $\Omega_c(css)/N_c$ compared to the chemical equilibrium (red, dashed line) expectation for regular hadronization temperature. We expect more than one percent of total charm yield to be found in $\Omega_c(css)$ state.

D. Yields of hadrons with two heavy quarks

We consider multi-heavy hadrons listed in the table III. The yields we will compute are now more model dependent since we cannot completely reduce the result, it either remains dependent on the reaction volume, or on the total charm yields. For example the yields of hadrons with two heavy quarks are approximately proportional to $1/dV/dy$ because $\gamma_{b,c}^H$ for heavy quarks is proportional to $1/dV/dy$, see Eq. (11):

$$\frac{dN_{hid}}{dy} \propto \gamma_c^H \frac{dV}{dy} \propto \frac{1}{dV/dy}, \quad (16)$$

$$\frac{dN_{Bc}}{dy} \propto \gamma_c^H \gamma_b^H \frac{dV}{dy} \propto \frac{1}{dV/dy}. \quad (17)$$

Moreover, as noted earlier the micro-canonical correction does not cancel out in these states, adding to the uncertainty.

Thus the result we present must seen as a guiding the eye and demonstrating a principle. In figure 11 we show

TABLE III: Hidden charm and multi heavy hadron states considered. States in parenthesis are not known experimentally

hadron		mass(GeV)	g
$\eta_c(1S)$	$c\bar{c}$	2.9779	1
$J/\Psi(1S)$	$c\bar{c}$	3.0970	3
$\chi_{c0}(1P)$	$c\bar{c}$	3.4152	1
$\chi_{c1}(1P)$	$c\bar{c}$	3.5106	3
$h_c(1P)$	$c\bar{c}$	3.526	3
$\chi_{c2}(1P)$	$c\bar{c}$	3.5563	5
$\eta_c(2S)$	$c\bar{c}$	3.638	1
$\psi(2S)$	$c\bar{c}$	3.686	3
ψ	$c\bar{c}$	3.770	3
ψ	$c\bar{c}$	3.836	5
ψ	$c\bar{c}$	4.040	3
ψ	$c\bar{c}$	4.159	3
ψ	$c\bar{c}$	4.415	3
B_c	$b\bar{c}$	6.27	1
Ξ_{cc}	ccq	3.527	4
Ω_{cc}	ccs	(3.660)	2

the yield of hidden charm $c\bar{c}$ mesons (see table III) normalized by the square of charm multiplicity N_c^2 as a function of hadronization temperature T . We consider again cases with $s/S = 0.03$ (upper panel, solid line) and $s/S = 0.04$ (lower panel, solid line). The chemical equilibrium $c\bar{c}$ mesons yields are shown (dashed lines on both panels) for two different values of $dV/dy = 600 \text{ fm}^{-3}$ (upper panel) and $dV/dy = 800 \text{ fm}^{-3}$ (lower panel), both for $T = 200 \text{ MeV}$.

The yield of $c\bar{c}$ mesons is much smaller for $s/S = 0.04$ than in equilibrium for the same dV/dy for large range of hadronization temperatures. For $s/S = 0.03$ the effect is similar, but suppression is not as pronounced. This suppression occurs due to competition with the yield of strange-heavy mesons. The enhanced yield of D_s in effect depletes the pool of available charmed quark pairs, and fewer hidden charm $c\bar{c}$ mesons are formed. For particles with two heavy quarks the effect is larger than for hadrons with one heavy quark and light quark(s). A similar situation arises for the B_c meson yield, see in figure 12, where we see $B_c/N_c N_b$ ratio as a function of hadronization temperature T , for the same strangeness yield cases as discussed for the hidden charm meson yield. Despite this suppression in strangeness rich environment, the B_c meson yield continues to be larger than the yield of B_c produced in single NN collisions where the scale yield is at the level of $\sim 10^{-5}$, see cross sections for $b\bar{b}$ and B_c in [16] and in [17].

In figure 13 we show scaled yields of ccq and ccs baryons as a function of temperature. Upper panel shows aside of the equilibrium case (dashed and dash-dot lines) the yields for $s/S = 0.04$ (solid line and dot marked line, respectively) for $dV/dy = 800 \text{ fm}^{-3}$ for $T = 200 \text{ MeV}$. Lower panel is for $dV/dy = 600 \text{ fm}^{-3}$ and $s/S = 0.03$. For the ccq baryons the suppression effect is the same as for $c\bar{c}$ and B_c mesons, equilibrium yield is much larger than non-equilibrium. But yield of ccs baryons is almost

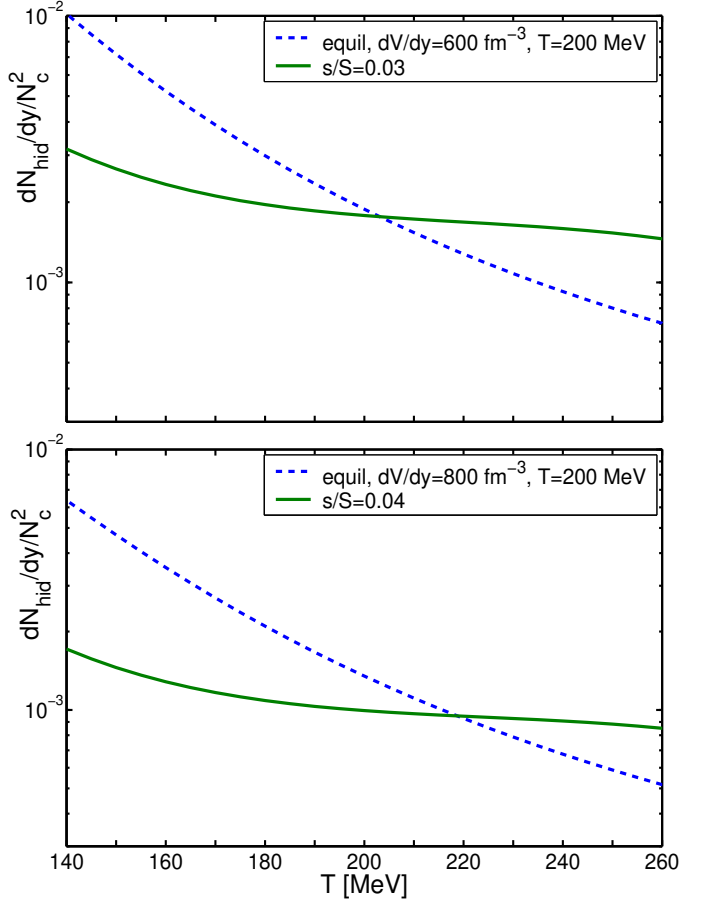


FIG. 11: (Color on line) $c\bar{c}/N_c^2$ states yields as a function of hadronization temperature T for the chemical equilibrium case with $dV/dy = 600 \text{ fm}^{-3}$ for $T = 200 \text{ MeV}$ (the upper panel, dashed line), for $s/S = 0.03$ with $dV/dy = 600 \text{ fm}^{-3}$ for $T = 200 \text{ MeV}$ (the upper panel, solid line), for chemical equilibrium case with $dV/dy = 800 \text{ fm}^{-3}$ for $T = 200 \text{ MeV}$ (the lower panel, dashed line) for $s/S = 0.04$ $dV/dy = 800 \text{ fm}^{-3}$ for $T = 200 \text{ MeV}$ (lower panel, solid line).

the same in equilibrium and $s/S = 0.04$ cases. The suppression effect is canceled by enhancement due to the presence of a strange quark.

V. CONCLUSIONS

We have considered here in some detail the abundances of heavy flavor hadrons within the statistical hadronization model. While we compare the yields to the expectations based on chemical equilibrium yields of light and strange quark pairs, we present results based on the hypothesis that the QGP entropy and QGP flavor yields determine the values of phase space occupancy γ_i^H $i = q, s, c, b$, which are of direct interest in study of the heavy hadron yields.

For highest energy heavy ion collisions the range of values discussed in literature is $1 \leq \gamma_q^H \leq 1.65$ and

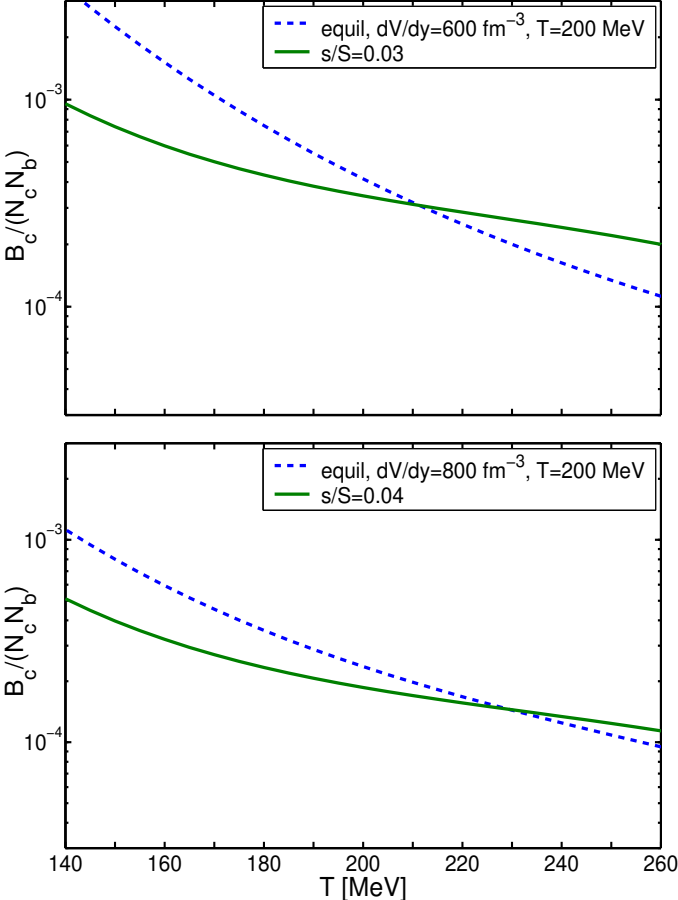


FIG. 12: (Color on line) B_c mesons yields as function of T for chemical equilibrium case with $dV/dy = 600 \text{ fm}^{-3}$ for $T = 200 \text{ MeV}$ (the upper panel, dashed line), for $s/S = 0.03$ with $dV/dy = 600 \text{ fm}^{-3}$ for $T = 200 \text{ MeV}$ (the upper panel, solid line), for chemical equilibrium case with $dV/dy = 800 \text{ fm}^{-3}$ for $T = 200 \text{ MeV}$ (the lower panel, dashed line) for $s/S = 0.04$ $dV/dy = 800 \text{ fm}^{-3}$ for $T = 200 \text{ MeV}$ (lower panel, solid line)

$0.7 \leq \gamma_s^H/\gamma_q^H \leq 1.5$. However γ_c^H and γ_b^H values which are much larger than unity arise. This is due to the need to describe the large primary parton based production, and considering that the chemical equilibrium yields are suppressed by the factor $\exp(-m/T)$.

Our work is based on grand canonical treatment of the phase space. That means that implicitly we assume a sufficiently large heavy flavor yield. This is true for charm, and the small corrections, as we have discussed are immaterial. Even though the yields of bottom heavy hadrons are subject to canonical suppression, this renormalizes the value of γ_b and in effect all single bottom hadrons can be explored within the grand canonical method, in so far we consider relative yield to a given initial bottom quark yield. Specifically, the canonical suppression does not influence the scaled yields of particles with one b quark i.e. B/N_b , B_s/N_b , B_c/N_b , etc. However for $b\bar{b}$ mesons and double b baryons the canonical effects should

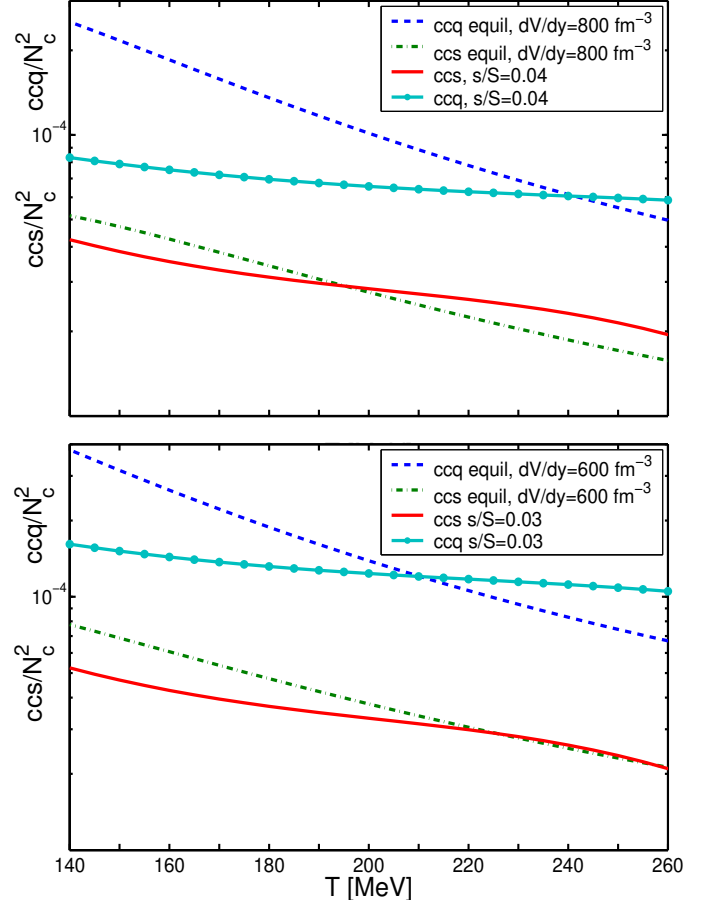


FIG. 13: (Color on line) ccq/N_c^2 and ccs/N_c^2 baryon yields as function of T . Upper panel: Chemical equilibrium case with $dV/dy = 1000 \text{ fm}^{-3}$ for $T = 200 \text{ MeV}$ (dashed line), $s/S = 0.04$ with $dV/dy = 800 \text{ fm}^{-3}$ for $T = 200 \text{ MeV}$ (solid line); and lower panel: chemical equilibrium case with $dV/dy = 600 \text{ fm}^{-3}$ for $T = 200 \text{ MeV}$ (dashed line), and $s/S = 0.03$ $dV/dy = 600 \text{ fm}^{-3}$ for $T = 200 \text{ MeV}$ (solid line).

be taken into account. Consideration of the yields of these particles is thus postponed.

We address here in particular how the yields of heavy hadrons are influenced by $\gamma_s^H/\gamma_q^H \neq 1$. The actual values of γ_s^H/γ_q^H we use are related to the strangeness per entropy yield s/S established in the QGP phase. Because the final value s/S is established well before hadronization, and the properties of the hadron phase space are well understood, the resulting γ_s^H/γ_q^H are well defined and turn out to be quite different from unity in the range of temperatures in which we expect particle freeze-out to occur. We consider in some detail the effect of QGP hadronization on the values of γ_s^H and γ_q^H , and note that the relative yield ϕ/K is independent of hadronization temperature when s/S is fixed by the conditions in the source.

Our first result we present allows a test of the statistical hadronization model for heavy flavor: we show that the yield ratio $c\bar{c} s\bar{s}/(c\bar{s} \bar{c}s)$ is nearly independent

of temperature and it is also nearly constant when the ϕ is allowed to freeze-out later, provided that the condition of production is at the same value of strangeness per entropy s/S .

We studied how the (relative) yields of strange and non-strange charmed mesons vary with strangeness content. For a chemically equilibrated QGP source, there is considerable shift of the yield from non-strange D to the strange D_s . Since the expected fractional yield $D_s/N_c \simeq B_s/N_b \simeq 0.2$ when one assumes $\gamma_s^H = \gamma^{H_q} = 1$, one should be able to falsify this hypothesis easily: the expected enhancement of the strange heavy mesons being at the level of 40% when $s/S = 0.03$, and greater when greater strangeness yield is available.

A consequence of this result is that we find a relative suppression of the multi-heavy hadrons, except when they contain strangeness. The somewhat ironic situation is that while higher charm QGP yield enhances production of $c\bar{c}$ states, enhanced strangeness suppresses this almost by that much. This new phenomenon adds to the complexity of interpretation of hidden charm meson yield. On the other hand, the yield of $c\bar{c}/N_c^2 \simeq 10^{-3}$ is found to be almost independent on hadronization temperature. The same is found for $B_c \approx 2 - 3 \cdot 10^{-4} N_c N_b$, that yield remains considerably larger than the scaled yield in single nucleon nucleon collisions.

We have shown that the study of heavy flavor hadrons will provide important information about the nature and properties of the QGP hadronization. The yield of $B_c(b\bar{c})$ mesons remains enhanced while the hidden charm $c\bar{c}$ states encounter another suppression mechanism, compensating for the greatly enhanced production due to large charm yield.

Acknowledgments

Work supported by a grant from: the U.S. Department of Energy DE-FG02-04ER4131. JR would like to thank F. Antinori for valuable comments regarding detection of D and D_s mesons.

APPENDIX A: ENTROPY

1. Entropy in QGP fireball

The entropy content is seen in the final state multiplicity of particles produced after hadronization. More specifically, there is a relation between entropy and particles multiplicities, once we note that the entropy per particle in a gas is:

$$\frac{S_B}{N} = 3.61, \quad \frac{S_{cl}}{N} = 4, \quad \frac{S_F}{N} = 4.2, \quad (A1)$$

for massless Bose, classical (Boltzmann) and Fermi gases, respectively. Effectively, for QGP with u, s, d, G degrees

of freedom, $S^Q/N^Q \sim 4$ is applicable for large range of masses. Thus:

$$\frac{dS^Q}{dy} \approx 4 \frac{dN^Q}{dy}. \quad (A2)$$

This in turn means that final state particle multiplicity provides us with information about the primary entropy content generated in the initial state of the QGP phase.

It is today generally believed that there is entropy conserving hydrodynamic expansion of the QGP liquid. Entropy is conserved in the fireball, and the conservation of entropy density σ flow is expressed by:

$$\frac{\partial_\mu(\sigma u^\mu)}{\partial x^\mu} = 0, \quad (A3)$$

where u^μ is local four velocity vector. A special case of interest is the so-called Bjørken scenario [18] for which Eq. (A3) can be solved exactly assuming as initial condition scaling of the physical properties as a function of rapidity. This implies that there is no preferred frame of reference, a situation expected in very high energy collisions. Even if highly idealized, this simple reaction picture allows a good estimate of many physical features. Of relevance here is that the exact solution of hydrodynamics in (1+1) dimensions implies

$$\frac{dS}{dy} = \text{Const.} \quad (A4)$$

Thus entropy S is not only conserved globally in the hydrodynamic expansion, but also per unit of rapidity. Though we have (1+3) expansion, Eq.(A4) holds as long as there is, in rapidity, a flat plateau of particles yields. Namely, each of the domains of rapidity is equivalent, excluding the projectile-target domains. However, at RHIC and LHC energies these are causally disconnected from the central rapidity bin, where we study the evolution of heavy flavor. The entropy we observe in the final hadron state has been to a large extent produced after the heavy flavor is produced, during the initial parton thermalization phase, but before strangeness has been produced. In order to model production of hadrons for different chemical freeze-out scenarios of the same reaction, we need to relate the entropy content, temperature and volume of the QGP domain. We consider for a u, d, G -chemically equilibrated QGP, and allowing for partial chemical equilibration of strangeness, the entropy content.

The entropy density σ can be obtained from: from the equation

$$\sigma \equiv \frac{S}{V} = -\frac{1}{V} \frac{dF_Q}{dT}, \quad (A5)$$

where the thermodynamic potential is:

$$F_Q(T, \lambda_q, V) = -T \ln Z_{(Q)T, \lambda_q, V}. \quad (A6)$$

Inside QGP the partition function is a product of partition function of gluons Z_g , light quarks Z_q and strange quarks Z_s , hence:

$$\ln Z = \ln Z_g + \ln Z_q + \ln Z_s; \quad (A7)$$

where for massless particles with $\lambda_q = 1$

$$\ln Z_g = \frac{g_g \pi^2}{90} V T^3, \quad (\text{A8})$$

$$\ln Z_q = \frac{7 g_q \pi^2}{4 \cdot 90} V T^3. \quad (\text{A9})$$

Here g_g is degeneracy factor for gluons and g_q is degeneracy factor for quarks. The factor $7/4 = 2 \cdot 7/8$ accounts for the difference in statistics and presence of both quarks and antiquarks. The number of degrees of freedom of quarks and gluons is influenced by strongly interactions, characterized by strong coupling constant α_s :

$$g_g = 2_s 8_c \left(1 - \frac{15}{4\pi} \alpha_s + \dots \right); \quad (\text{A10})$$

$$g_q = 2_s 3_c 2_f \left(1 - \frac{50}{21\pi} \alpha_s + \dots \right). \quad (\text{A11})$$

The case of strange quarks is somewhat more complicated, since we have to consider the mass, the degree of chemical equilibration, and guess-estimate the strength of QCD perturbative interactions. We have in Boltzman approximation:

$$\ln Z_s = 2_{\text{p/a}} \frac{g_s}{\pi^2} V T^3, \quad (\text{A12})$$

$$g_s = 2_s 3_c \gamma_s^Q 0.5 W(m_s/T) \left(1 - k \frac{\alpha_s}{\pi} \right). \quad (\text{A13})$$

$W(m/T)$ is function seen in Eq. (4). We allow both for strange and antistrange quarks, factor $2_{\text{p/a}}$ (which is for massless fermions $2 \cdot 7/8 = 7/4$). k at this point is a temperature dependent parameter. Even in the lowest order perturbation theory it has not been evaluated for massive quarks at finite temperature. We know that for massless quarks $k \simeq 2$. Considering expansion in m/T , for large masses the correction reverses sign [19], which result supports the reduction in value of k for $m \simeq T$. We will use here the value $k = 1$ [10].

2. Number of degrees of freedom in QGP

The entropy density following from Eq. (A5) is:

$$\sigma = \frac{4\pi^2}{90} (g_g + \frac{7}{4} g_q) T^3 + \frac{4}{\pi^2} 2_{\text{p/a}} g_s T^3 + \frac{\mathcal{A}}{T}. \quad (\text{A14})$$

For strange quarks in the second term in Eq. (A14) we set the entropy per strange quarks to 4 units. In choosing $S_s/N_s = 4$ irrespective of the effect of interaction and mass value m_s/T we are minimizing the influence of unknown QCD interaction effect.

The last term in Eq. (A14) comes from differentiation of the strong coupling constant α_s in the partition function with respect to T , see Eq.(A5). Up to two loops in the β -function of the renormalization group the correction term is [20]:

$$\mathcal{A} = (b_0 \alpha_s^2 + b_1 \alpha_s^3) \left[\frac{2\pi}{3} T^4 + \frac{n_f 5\pi}{18} T^4 \right] \quad (\text{A15})$$

with n_f being the number of active fermions in the quark loop, $n_f \simeq 2.5$, and

$$b_0 = \frac{1}{2\pi} \left(11 - \frac{2}{3} n_f \right), \quad b_1 = \frac{1}{4\pi^2} \left(51 - \frac{19}{3} n_f \right). \quad (\text{A16})$$

For the strong coupling constant α_s we use

$$\alpha_s(T) \simeq \frac{\alpha_s(T_c)}{1 + C \ln(T/T_c)}, \quad C = 0.760 \pm 0.002, \quad (\text{A17})$$

where $T_c = 0.16$ GeV. This expression arises from renormalization group running of $\alpha_s(\mu)$, the energy scale at $\mu = 2\pi T$, and the value $\alpha_s(M_Z) = 0.118$. A much more sophisticated study of the entropy in the QGP phase is possible [21], what we use here is an effective model which agrees with the lattice data [22].

Eq. (A14) suggest that we introduce an effective degeneracy of the QGP based on the expression we use for entropy:

$$g_{\text{eff}}^Q(T) = g_g(T) + \frac{7}{4} g_q(T) + 2g_s \frac{90}{\pi^4} + \frac{\mathcal{A}}{T^4} \frac{90}{4\pi^2}. \quad (\text{A18})$$

Which allows us to write:

$$\sigma = \frac{4\pi^2}{90} g_{\text{eff}}^Q T^3, \quad (\text{A19})$$

and

$$\frac{dS}{dy} = \frac{4\pi^2}{90} g_{\text{eff}}^Q T^3 \frac{dV}{dy} \simeq \text{Const.} \quad (\text{A20})$$

We show the QGP degeneracy in figure 14, as a function of $T \in [140, 260]$ MeV, top frame for fixed $s/S = 0, 0.03, 0.04$ (from bottom to top), and in the bottom frame for the strangeness chemical equilibrium, $\gamma_s = 1$ (dashed) and approach to chemical equilibrium cases (solid). When we fix the specific strangeness content s/S in the plasma comparing different temperatures we find that in all cases g_{eff}^Q increases with T . For $s/S = 0$ we have a 2-flavor system (dotted line, red) and the effective number of degrees of freedom g_{eff}^Q varies between 22 and 26. The solid line with dots (green) is for $s/S = 0.03$, and the dot-dashed line (blue) gives the result for $s/S = 0.04$.

In the bottom panel of figure 14 we note that like for 2 flavors, case (s=0), for the 2+1-flavor system ($\gamma_s = 1$) g_{eff}^Q increases with T (dashed line, black). g_{eff}^Q varies between 30 and 35.5. The thin dashed lines indicate the range of uncertainty due to mass of the strange quark, which in this calculation is fixed with upper curve corresponding to $m_s = 90$ MeV, and lower one $m_s = 160$ MeV. The expected decrease in value of m_s with T will thus have the effect to steepen the rise in the degrees of freedom with T .

We now explore in a QGP phase the effect of an increasing strangeness fugacity with decreasing temperature. This study is a bit different from the rest of this paper, where we consider for comparison purposes

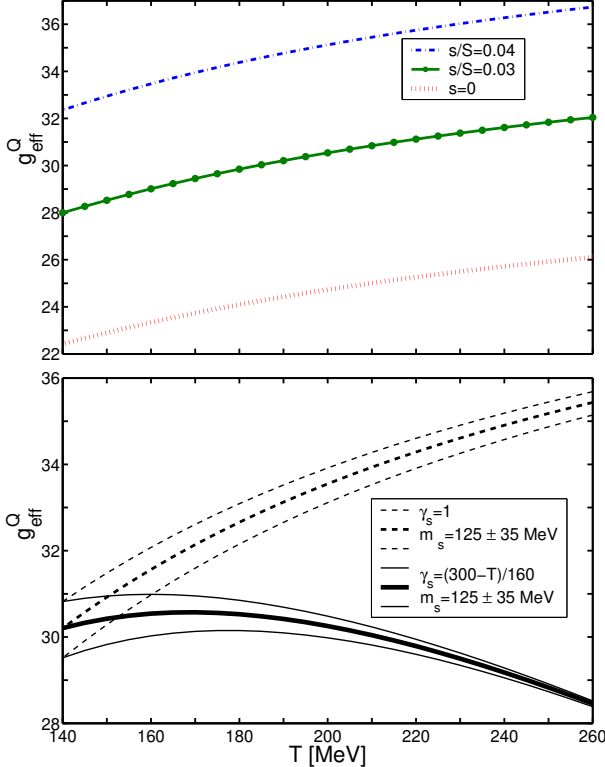


FIG. 14: (color on-line) The Stefan-Boltzmann degrees of freedom g_{eff}^Q based on entropy content of QGP, as function of temperature T . Upper frame: fixed s/S , the solid line with dots (green) is for a system with fixed strangeness per entropy $s/S = 0.03$, while dot-dashed (blue) line is for $s/S = 0.04$. The dotted (red) line is for 2-flavor QCD $s/S = 0$ (u, d, G only); The bottom frame shows dashed (black) line 2+1-flavor QCD with $m_s = 125 \pm 35$ MeV (chemically equilibrated u, d, s, G system). The (thick, thin) solid lines are for QGP in which strangeness contents is increasing as function of temperature, see text.

hadronization for a range of temperatures but at a *fixed* value of s/S . A variable $\gamma_s^Q(T)$ implies a more sophisticated, and thus more model dependent picture of plasma evolution. However, this offers us an important insight about g_{eff}^Q .

We consider the function:

$$\gamma_s^Q = \frac{300 - T[\text{MeV}]}{160}. \quad (\text{A21})$$

This is consistent with the kinetic computation of strangeness production [10]. At $T = 140$ MeV we have chemical equilibrium in the QGP phase, while and at the temperature $T = 260$ MeV we have $\gamma_s = 0.25$. The result for g_{eff}^Q is shown as a thick (black) line in figure 14, with the range showing strange quark mass range $m_s = 125 \pm 35$ MeV. We see that in a wide range of temperatures we have $29.5 < g_{\text{eff}}^Q < 30.5$.

The lesson is that with the growth of γ_s^Q with decreasing T the entropy of the QGP is well described

TABLE IV: Reference values of volume, temperature, entropy, particle multiplicity

$dV/dy [\text{fm}^3]$	$T[\text{MeV}]$	dS^Q/dy	dN^Q/dy	dN^H/dy
800	200	10,970	2,700	5,000
2300	140	10,890	2,700	4,500

by a constant value $g_{\text{eff}}^Q = 30 \pm 0.5$. Since the entropy is (nearly) conserved and g_{eff}^Q is (nearly) constant, Eq. (A20) implies that we can scale the system properties using $T^3 dV/dy = \text{Const}$. We stress again that these results arises in a realistic QGP with $2 + \gamma_s^Q$ -flavors, but are model dependent and of course rely on the lattice motivated description of the behavior of QGP properties. On the other hand it is not surprising that the rise of strangeness chemical saturation with decreasing temperature compensates the ‘freezing’ or ‘strong interaction sticking’ of the q, G -degrees of freedom with decreasing temperature.

3. Entropy content and chemical (non)equilibrium

We use as a reference a QGP state with $dV/dy = 800 \text{ fm}^3$ at $T = 200 \text{ MeV}$, see table IV. We find from Eq. (A2) the Q and H phase particle multiplicity. The hadron multiplicity stated is what results after secondary resonance decays. The total hadron multiplicity after hadronization and resonance decays was calculated using on-line SHARE 1.2 [23]. If a greater (smaller) yield of final state hadrons is observed at LHC, the value of dV/dy need to be revised up (down). In general expansion before hadronization will not alter dS/dy . We can expect that as T decreases, $V^{1/3}$ increases. Stretching the validity of Eq. (A20) to low temperature $T = 140 \text{ MeV}$, we see the result in the second line of table IV.

For QGP, in general the entropy content is higher than in a comparable volume of chemically equilibrated hadron matter, because of the liberation of color degrees of freedom in the color-deconfined phase. The total entropy has to be conserved during transition between QGP and HG phases, and thus after hadronization, the excess of entropy is observed in excess particle multiplicity, which can be interpreted as a signature of deconfinement [24, 25]. The dynamics of the transformation of QGP into HG determines how this additional entropy manifests itself.

The comparison of entropy in both phases is temperature dependent but in the domain of interest i.e. $140 < T < 180 \text{ MeV}$ the entropy density follows:

$$\sigma^Q \gtrsim 3\sigma^H. \quad (\text{A22})$$

Since the total entropy S is conserved or slightly increases, in the hadronization process some key parameter must grow in the hadronization process. There are two options:

a) either the volume changes:

$$3V^H \gtrsim V^Q; \quad (\text{A23})$$

or

b) the phase occupancies change, and since $n_i \propto \gamma_i^{2,3}$, $i = q, s$ in hadron phase

$$\gamma_q^H \simeq \sqrt{3}, \quad \gamma_s^H / \gamma_q^H \gtrsim 1. \quad (\text{A24})$$

In a slow, on hadronic time scale, transition, such as is the case in the early Universe, we can expect that case a) prevails. In high energy heavy ion collisions, there is no evidence in the experimental results for the long coexistence of hadron and quark phases which is required for volume growth. Consequently, we have $V^H \sim V^Q$ and a large value of γ_q^H is required to conserve entropy. The value of γ_q^H is restricted by

$$\gamma_q^{\text{cr}} \cong \exp(m_\pi^0/2T). \quad (\text{A25})$$

This value γ_q^{cr} is near to maximum allowed value, which arises at condition of Bose-Einstein condensation of pions. We will discuss quantitative results for γ_q^H (and γ_s^H) below in appendix B 3.

APPENDIX B: STRANGENESS

1. Abundance in QGP and HG

The efficiency of strangeness production depends on energy and collision centrality of heavy ions collisions. The increase, with value of centrality (participant number), of per-baryon specific strangeness yield indicates presents of strangeness production mechanism acting beyond the first collision dynamics. The thermal gluon fusion to strangeness can explain this behavior [8], and a model of the flow dynamics at RHIC and LHC suggests that the QGP approaches chemical equilibrium but also can exceed it at time of hadronization [10].

The strangeness yield in chemically equilibrated QGP is usually described as an ideal Boltzmann gas. However, a significant correction is expected due to perturbative QCD effects. We implement this correction based on comments below Eq. (A13). We use here the expression:

$$\frac{dN_s^Q}{dy} = \gamma_s^Q \left(1 - \frac{\alpha_s}{\pi}\right) n_s^{\text{eq}} \frac{dV}{dy}. \quad (\text{B1})$$

with the Boltzmann limit density Eq. (3), and mass $m_s = 125 \text{ MeV}$, $g_s = 6$, $\lambda_s = 1$. The QCD correction corresponds to discussion of entropy in appendix A 1

We obtain strange quarks phase space occupancy γ_s^H as function of temperature from condition of equality of the number of strange quark and antiquark pairs in QGP and HG. Specifically, in the sudden QGP hadronization, quarks recombine and we expect that the strangeness content does not significantly change. For heavier flavors across the phase boundary this condition Eq. (7) is

very well satisfied, for strangeness the fragmentation phenomenon adds somewhat to the yield,

$$\frac{dN_s^H}{dy} \gtrsim \frac{dN_s^Q}{dy}. \quad (\text{B2})$$

Using the equality of yields we underestimate slightly the value of strangeness occupancy that results. We recall that we also conserver entropy Eq. (8) which like strangeness can in principle grow in hadronization,

$$\frac{s}{S} \Big|_H \gtrsim \frac{s}{S} \Big|_Q. \quad (\text{B3})$$

using Eq. (8) we underestimate the value of γ_q^H .

Counting all strange particles, the number of pairs is:

$$\begin{aligned} \frac{dN_s^H}{dy} = \frac{dV}{dy} & [\gamma_s^H (\gamma_q^H n_{K^+}^{\text{eq}} + \gamma_q^H n_{K^0}^{\text{eq}}) \\ & + \gamma_s^H (2\gamma_q^H n_{\Xi}^{\text{eq}} + n_\phi^{\text{eq}} + P_s n_\eta^{\text{eq}}) \\ & + 3\gamma_s^H n_\Omega^{\text{eq}}], \end{aligned} \quad (\text{B4})$$

where n_i^{eq} are densities of strange hadrons (mesons and baryons) calculated using Eq. (2) in chemical equilibrium. P_s is the strangeness content of the η . The way we count hadrons is to follow strangeness content, for example $n_K^{\text{eq}} = n_{K^+}^{\text{eq}} + n_{K^0}^{\text{eq}} = n_{K^-}^{\text{eq}} + n_{\bar{K}^0}^{\text{eq}}$. We impose in our calculations $\bar{s} = s$. The pattern of this calculation follows an established approach, SHARE 1.2 [23] was used in detailed evaluation.

2. Strangeness per entropy s/S

Considering that both strangeness, and entropy, are conserved in the hadronization process, a convenient variable to consider as fixed in the hadronization process, is the ratio of these conserved quantities s/S . In chemical equilibrium we expect that in general such a ratio must be different for different phases of matter from which particles are produced [10, 26, 27].

We compare QGP and HG specific per entropy strangeness content in figure 15. We show as function of temperature T the s/S ratios for chemically equilibrated QGP and HG phase. For the QGP the entropy S in QGP is calculated as described in appendix A, and we use $k = 1$ in Eq. (B1). The shaded area shows the range of masses of strange quarks, considered, results for $m_s = 90 \text{ MeV}$ (upper (blue) dash-dotted line) and $m_s = 160 \text{ MeV}$ ((green) solid line) form the boundaries. The central QGP value is at about $s/S = 0.032$.

The short-dashed (light blue) line shows the hadron phase s/S value found using SHARE 1.2. For HG near to usual range of hadronization temperature $T \simeq 160 \text{ MeV}$ we find $s/S \simeq 0.025$. In general formation of QGP implies and increase by 30% in s/S . Both HG and QGP phases have a similar specific strangeness content at $T = 240\text{--}260 \text{ MeV}$, however it is not believed that a HG

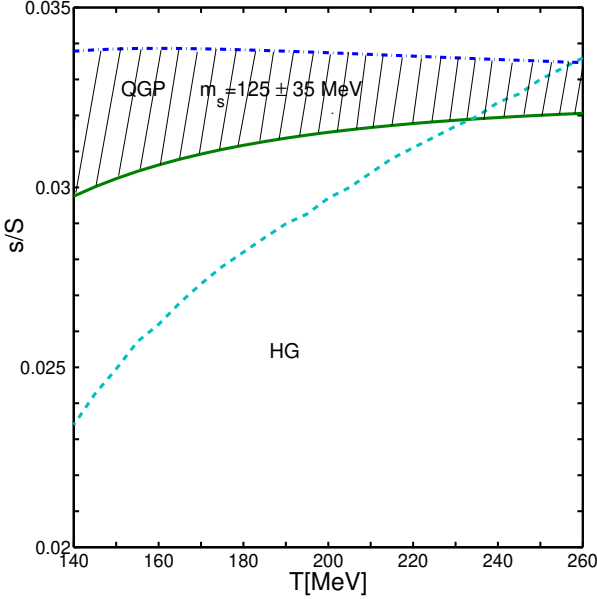


FIG. 15: (Color on line) Strangeness to entropy ratio s/S as function of temperature T , for the QGP (green, solid line for $m_s = 160$ MeV, blue dash-dot line for $m_s = 90$ MeV) with $k = 1$, see Eq. (B1); and for HG (light blue, dashed line) phases for $\gamma_q = \gamma_s = \lambda_q = \lambda_s = 1$ in both phases.

at such high temperature would be a stable form of matter. This HG to QGP dissociation, or QGP hadronization depends on the degree of strangeness equilibration in plasma [28], and other dynamical factors.

In the QGP the value of s/S for the range of realistic hadronization temperature $140 < T < 180$ MeV is in general larger than in HG. This implies that generally, the abundance of strange hadrons produced in hadronization over saturates the strange hadron phase space, if QGP state had reached (near) chemical equilibrium. Moreover, since we are considering the ratio s/S and find in QGP a value greater than in HG, for chemical equilibrium in QGP the hadronization process will lead to $\gamma_s^H/\gamma_q^H > 1$.

One can wonder if we have not overlooked some dynamical or microscopic effect which could adjust the value of s/S implied by QGP to the value expected in HG. First we note that the fast growth of the volume V cannot change s/S . Moreover, any additional strangeness production in hadronization would enhance the over-abundance recorded in the resulting HG. Only a highly significant entropy production at fixed strangeness yield in the hadronization process could bring the QGP s/S ratio down, masking strangeness over-saturation. A mechanism for such entropy production in hadronization is unknown, and moreover, this would further entail an unexpected and high hadron multiplicity excess.

One could of course argue that the perturbative QCD properties in the QGP are meaningless, the entropy in QGP is much higher at given temperature. However, the properties of QGP have been checked against the lattice results, and the use of lowest order expressions is

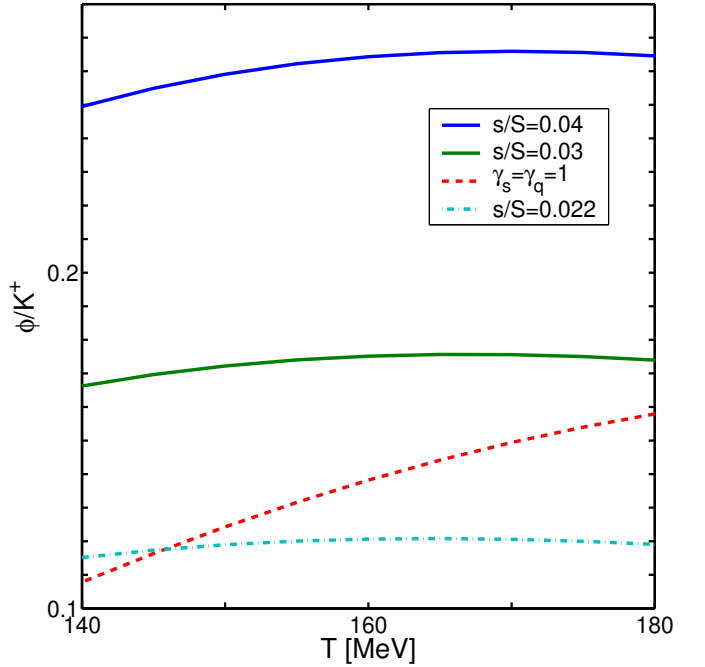


FIG. 16: (Color on line) The ratio ϕ/K^+ as function of T . Dashed line (red) is for chemical equilibrium. Solid line with dots (green) $s/S = 0.03$, solid line (blue) $s/S = 0.04$, dash-dot line (per) is for $s/S = 0.022$.

justified in these terms [22]. Moreover, the value of s/S is established way before hadronization.

One of course would like to measure the value of s/S irrespective of what the hadronization temperature may be. We find that the ratio ϕ/K^+ is very insensitive to hadronization temperature and is relatively strongly dependent on the value of s/S . In figure 16 we consider the hadron phase space ratio ϕ/K^+ as function of T for different s/S ratios, and for $\gamma_s = 1$ chemical equilibrium (dashed line). The K^+ yield contains the contribution from the decay of ϕ into kaons which is a noticeable correction.

The reason that this ratio ϕ/K^+ is practically a constant as function of T for s/S fixed is recognized considering that it is a product of two factors,

$$\frac{\phi}{K^+} = \frac{\gamma_s^H}{\gamma_q^H} \frac{n_\phi^{\text{eq}}}{n_{K^+}^{\text{eq}}} \quad (\text{B5})$$

In figure 18 we have seen that at fixed s/S the first factor γ_s^H/γ_q^H rises exponentially with decreasing T . It so happens that the rise is exactly compensated by the corresponding exponential decrease associated with the non-relativistic limit of the equilibrium hadron ratio, see Eq. (5).

We record in table V for given s/S and volume dV/dy the corresponding total yields of strangeness, which may be useful in consideration of the consistency of experimental results with what we find exploring heavy flavor hadron abundance.

TABLE V: Specific and absolute strangeness yield for different reaction volumes at $T = 200$.

s/S	ds/dy	dV/dy [fm $^{-3}$]	T [MeV]
0.04	560	800	200
0.03	240	600	200
0.022	95	400	200

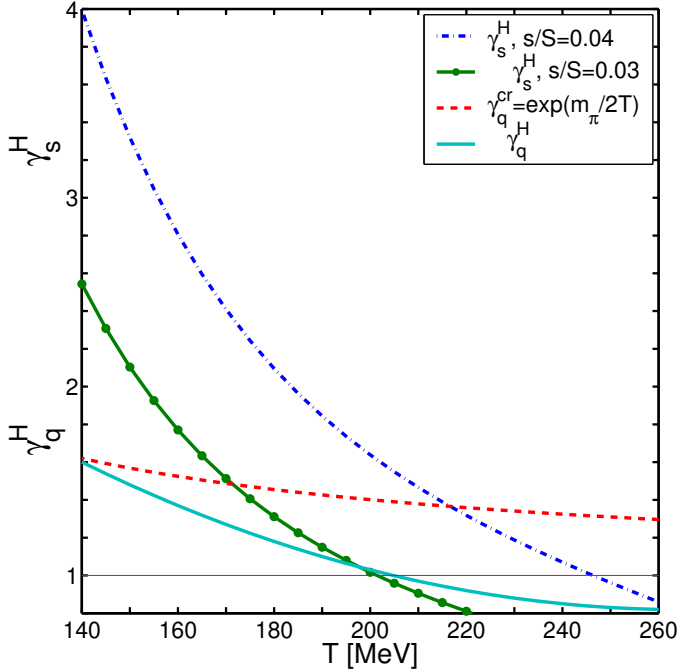


FIG. 17: (color on-line) Phase space occupancy as function of T : γ_q^H (blue, solid line), γ_s^H for $s/S = 0.03$ (green, line with point markers) and for $s/S = 0.04$ (blue, dash-dotted line); γ_q^{cr} (red, dashed line).

3. Strangeness chemical non-equilibrium

In order that in fast hadronization there is continuity of strangeness Eq. (B2), and entropy, Eq. (B3) the hadron phase $\gamma_s^H \neq 1$ and $\gamma_q^H \neq 1$. We have to solve for γ_s^H and γ_q^H simultaneously Eqs. (B2,B3).

Quantitative results for γ_q^H and γ_s^H are shown in figure 17. The maximum allowed value Eq. (A25) is shown dashed (red) line. The actual value of γ_q^H (solid line, blue on-line) reaches the maximum value dashed (red) line, Eq. (A25) near to $T = 140$ MeV. For $T > 200$ MeV the entropy content in the hadron phase is greater than in QGP, as is seen by the value $\gamma_q^H < 1$. however, it is not generally believed that the HG phase can exist at such high temperature.

The results we present in figure 17, are for a fixed value of s/S (strangeness pair yield per entropy) which is established in the QGP phase. For the chemical equilibrium QGP strangeness content $s/S = 0.03$ the strangeness oc-

cupancy $\gamma_s^H > \gamma_q^H$ for $T < 200$ MeV. We also show phase space occupancy γ_s^H for $s/S = 0.04$ (blue, dash-dotted line). This large QGP strangeness content would lead to large values of $\gamma_s^H > 5$, for $T < 150$ MeV.

In figure 18 top panel we show the ratio γ_s^H/γ_q^H at three values of s/S . Except in case that strangeness were to remain well below chemical equilibrium in QGP ($s/S = 0.022$), the abundance of heavy flavor hadrons we turn to momentarily will be marked by an overabundance of strangeness, since practically in all realistic conditions we find $\gamma_s^H > \gamma_q^H$.

In the bottom panel of figure 18 we force the chemical equilibrium of light quarks $\gamma_q^H = 1$. This is a (at RHIC, LHC unlikely) scenario in which hadronization is slow and/or a mixed phase develops. What we see is that the high QGP strangeness content is in this condition more visible.

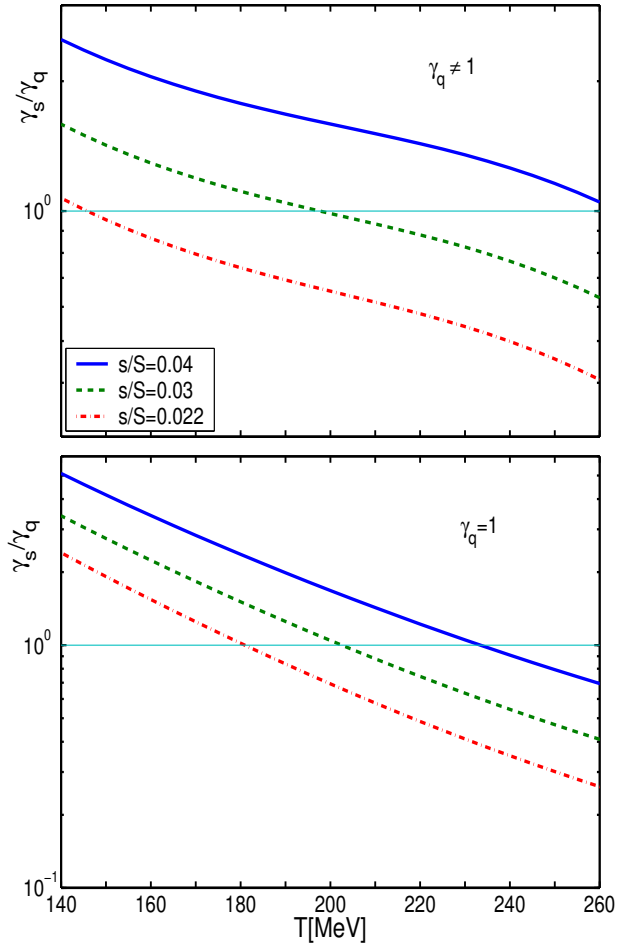


FIG. 18: (color on line) γ_s^H/γ_q^H as function of hadronization temperature T for (from top to bottom) $s/S = 0.04$ (blue, solid line), $s/S = 0.03$ (green, dashed line), $s/S = 0.022$ (red, dash-dotted line). Upper panel for $\gamma_q^H \neq 1$, lower panel for $\gamma_q^H = 1$.

[1] K. Geiger, Phys. Rev. D **48**, 4129 (1993).

[2] M. Cacciari, P. Nason and R. Vogt, Phys. Rev. Lett. **95**, 122001 (2005) [arXiv:hep-ph/0502203].

[3] H. van Hees and R. Rapp, Phys. Rev. C **71**, 034907 (2005) [arXiv:nucl-th/0412015].

[4] M. Schroedter, R. L. Thews and J. Rafelski, Phys. Rev. C **62**, 024905 (2000) [arXiv:hep-ph/0004041].

[5] F. Becattini, Phys. Rev. Lett. **95**, 022301 (2005) [arXiv:hep-ph/0503239].

[6] R. L. Thews, Eur. Phys. J. C **43**, 97 (2005) [arXiv:hep-ph/0504226].

[7] I. Kuznetsova and J. Rafelski, arXiv:hep-ph/0605307.

[8] P. Koch, B. Muller and J. Rafelski, Phys. Rept. **142**, 167 (1986).

[9] A. Andronic, P. Braun-Munzinger, K. Redlich and J. Stachel, Phys. Lett. B **571**, 36 (2003) [arXiv:nucl-th/0303036].

[10] J. Letessier and J. Rafelski, arXiv:nucl-th/0602047.

[11] E. Fermi, Prog. Theor. Phys. **5**, 570 (1950).

[12] R. Hagedorn, “How We Got To QCD Matter From The Hadron Side By Trial And Error,” CERN-TH-3918/84 *Invited talk given at Quark Matter 1984, 4th Int. Conf. on Ultrarelativistic Nucleus-Nucleus Collisions, Helsinki, Finland, Jun 17-21, 1984* K. Kajantie, ed. Springer-Verlag, Lecture Notes in Physics, 221, pp53-76.

[13] E. Cheu [the D0 collaboration], Int. J. Mod. Phys. A **20**, 3664 (2005).

[14] T. Matsuki and T. Morii, Phys. Rev. D **56**, 5646 (1997) [Austral. J. Phys. **50**, 163 (1997)] [arXiv:hep-ph/9702366].

[15] C. Albertus, J. E. Amaro, E. Hernandez and J. Nieves, Nucl. Phys. A **740**, 333 (2004) [arXiv:nucl-th/0311100].

[16] K. Anikeev *et al.*, “B physics at the Tevatron: Run II and beyond,” arXiv:hep-ph/0201071, SLAC-REPRINT-2001-056, FERMILAB-PUB-01-197, Dec 2001. 583pp. *Workshop on B Physics at the Tevatron: Run II and Beyond, Batavia, Illinois, 24-26 Feb 2000.*

[17] C. H. Chang and X. G. Wu, Eur. Phys. J. C **38**, 267 (2004) [arXiv:hep-ph/0309121].

[18] J. D. Bjorken, Phys. Rev. D **27**, 140 (1983).

[19] J. I. Kapusta, Nucl. Phys. B **148**, 461 (1979).

[20] S. Hamieh, J. Letessier and J. Rafelski, Phys. Rev. C **62** (2000) 064901 [arXiv:hep-ph/0006085].

[21] Joseph I. Kapusta, and Charles Gale, *Finite-Temperature Field Theory : Principles and Applications* Cambridge Monographs on Mathematical Physics, 2006, ISBN: 0521820820

[22] J. Letessier and J. Rafelski, Phys. Rev. C **67**, 031902 (2003) [arXiv:hep-ph/0301099]; J. Rafelski and J. Letessier, Nucl. Phys. A **702**, 304 (2002) [arXiv:hep-ph/0112027].

[23] G. Torrieri, S. Steinke, W. Broniowski, W. Florkowski, J. Letessier and J. Rafelski, Comput. Phys. Commun. **167**, 229 (2005) [arXiv:nucl-th/0404083].

[24] J. Letessier, A. Tounsi, U. W. Heinz, J. Sollfrank and J. Rafelski, Phys. Rev. Lett. **70**, 3530 (1993) [arXiv:hep-ph/9711349].

[25] J. Letessier, A. Tounsi, U. W. Heinz, J. Sollfrank and J. Rafelski, Phys. Rev. D **51**, 3408 (1995) [arXiv:hep-ph/9212210].

[26] J. I. Kapusta and A. Mekjian, Phys. Rev. D **33** (1986) 1304.

[27] J. Letessier, J. Rafelski and A. Tounsi, Phys. Lett. B **323**, 393 (1994) [arXiv:hep-ph/9711345].

[28] J. Rafelski and J. Letessier, “Hadronization of Expanding QGP,” arXiv:nucl-th/0511016, The European Physics Journal A (2006) in press.